Robotica (2024), 1–33
doi:10.1017/S026357472400050X

CAMBRIDGE UNIVERSITY PRESS

RESEARCH ARTICLE

Multibody dynamics in robotics with focus on contact events

Mariana Rodrigues da Silva, Joana Coelho, Fernando Gonçalves, Francisco Novais and Paulo Flores

CMEMS-UMinho, Department of Mechanical Engineering, University of Minho, Guimarães, Portugal
Corresponding author: Paulo Flores; Email: pflores@dem.uminho.pt.

Received: 17 December 2023; **Revised:** 13 March 2024; **Accepted:** 22 March 2024

Keywords: multibody dynamics; robotic systems; contact events; contact detection; contact force models; friction force models

Abstract

Multibody dynamics methodologies have been fundamental tools utilized to model and simulate robotic systems that experience contact conditions with the surrounding environment, such as in the case of feet and ground interactions. In addressing such problems, it is of paramount importance to accurately and efficiently handle the large body displacement associated with locomotion of robots, as well as the dynamic response related to contact-impact events. Thus, a generic computational approach, based on the Newton–Euler formulation, to represent the gross motion of robotic systems, is revisited in this work. The main kinematic and dynamic features, necessary to obtain the equations of motion, are discussed. A numerical procedure suitable to solve the equations of motion is also presented. The problem of modeling contacts in dynamical systems involves two main tasks, namely, the contact detection and the contact resolution, which take into account for the kinematics and dynamics of the contacting bodies, constituting the general framework for the process of modeling and simulating complex contact scenarios. In order to properly model the contact interactions, the contact kinematic properties are established based on the geometry of contacting bodies, which allow to perform the contact detection task. The contact dynamics is represented by continuous contact force models, both in terms of normal and tangential contact directions. Finally, the presented formulations are demonstrated by the application to several robotics systems that involve contact and impact events with surrounding environment. Special emphasis is put on the systems' dynamic behavior, in terms of performance and stability.

1. Introduction

1.1. Purpose of this work

Multibody dynamics is a powerful tool for the systematic simulation, analysis, and optimization of the motion of mechanical systems and has a vast spectrum of application in several engineering areas. A multibody system is composed of three main ingredients, namely, a collection of interconnected rigid and/or flexible bodies describing large rotational and translational motions, joints that kinematically constrain the relative motion of the adjacent bodies, and force or driving elements acting upon those bodies. The Newton–Euler formulation is among the most widely utilized methodologies to model multibody robotic systems due to its simplicity and straightforward to apply in general-purpose codes, being the main approach adopted in this work. Integrating multibody dynamics formulations into the modeling and simulation of robotic systems can significantly improve the understanding of their behavior and performance, particularly in scenarios involving contacts and interactions of complex nature. This knowledge can be essential for the design, control, and optimization of robots that operate in real-world environments. Thus, the main purpose of this paper is to provide a comprehensive analysis of multibody dynamics in robotics, with particular focus on applications that involve contact-impact events. The presented approaches allow for an accurate representation of the dynamic response, contact forces, and

frictional effects, providing valuable insights for the design, analysis, and optimization of robotic systems. In the sequel of this process, the key ingredients associated with kinematic and dynamic aspects in multibody systems are revisited. Then, an overview of the main normal and tangential force models is offered. Finally, two robotics systems that involve contact-impact scenarios are used to demonstrated the presented methodologies.

1.2. Multibody dynamics in robotics

In the specific domain of robotics, multibody dynamics has emerged as a vital and widely employed approach for investigating and understanding the movement and dynamic responses of robots in diverse real-world scenarios [1, 2]. In fact, multibody dynamics provides an accurate representation of robotic behavior, in the measure that robotic systems typically consist of multiple interconnected bodies, linked by joints, and subjected to external forces. This is especially relevant considering the significant body displacement associated with the locomotion of robots [3, 4].

Over the past few decades, the analysis of robotic systems using multibody dynamics methodologies has been a subject of extensive investigation. Grazioso et al. [5] presented and validated a new passive articulated suspension tracked robot using multibody dynamics methodologies. For this purpose, the commercial software MSC Adams was utilized to develop the multibody model, which was considered in the design and optimization of the solution obtained. The performance of the multibody model was compared and validated with experimental data, being, subsequently, utilized to examine its effectiveness in different challenging environments. Mucchi and co-workers [6] validated a flexible multibody model of a commercial 3R planar manipulator. This manipulator consists of five rigid bodies and 11 massless parts interconnected by nine revolute joints. Flexibility was incorporated in the base and in the joints. In this study, the flexible multibody model was utilized to study low-frequency vibrations that can be generated during particular installation conditions of industrial serial planar manipulators. Bascetta et al. [7] developed a closed-form multibody dynamic model of flexible manipulators using the Newton–Euler formulation. In this investigation, the utilization of the Newton–Euler approach, articulated in terms of joint and elastic variables, not only enhances simulation performance but also makes the model well-suited for real-time control and active vibration damping. The multibody model was compared and validated with benchmarks from the literature obtained through the classical multibody approach. Additionally, further validation was conducted by comparing the model with experiments conducted on an experimental manipulator.

Chang and co-authors [8] modeled and developed a quadruped legged with the aim at identifying the dynamic parameters related to systems behavior. In this investigation, the Gazebo software was utilized to assess the performance of a quadruped robot with a total of 16 degrees-of-freedom. Vasileiou et al. [9] presented a unified framework to develop a passive robot using multibody dynamics for that purpose, being the computational results compared and validated with data collected from an experimental prototype. These authors demonstrated the effectiveness of using digital twin in the design and development process of walking robots [5, 10]. In turn, Kim et al. [11] proposed a method to simulate multibody robotic systems driven by DC motors, based on the Newton–Euler method, to account for the electromechanical coupling effects, which allows a more realistic and reliable prediction of the dynamic responses of such systems. The proposed model was utilized in the analysis of two robotic systems equipped with DC motors, namely an industrial robot and a flexible satellite antenna. Ingrosso et al. [12] developed a rigid multibody model of an underwater multi-hull vehicle to compute the lumped parameter hydrodynamic derivative matrices using the multibody approach.

Robotic technologies are also utilized in specific tasks that are difficult, repetitive, or unsafe for humans [13–15]. In this context, Kim et al. [16] adopted the Lagrange formulation and introduced a method for planning load-effective dynamic motions for redundant systems. The authors demonstrated the applicability of the proposed method in pulling tasks using a highly articulated 30 degrees-of-freedom human model of the torso and arms. Zhang and Zhang [17] designed and developed a lower limb exoskeleton robots' dynamics parameters identification based on improved beetle swarm optimization

https://doi.org/10.1017/S026357472400050X Published online by Cambridge University Press

algorithm, in which a beetle swarm optimization methodology was designed and utilized to identify the dynamics parameters of the robot system. The proposed approach was developed with basis on the beetle antennae search algorithm and particle swarm optimization. Experimental investigation carried out on an exoskeleton model was used to demonstrate the accuracy and effectiveness of the proposed solution. More recently, Gonçalves et al. [18, 19] developed a human-like mobile domestic robot, called CHARMIE, to improve the healthcare and quality of life of elderly people by performing household chores. The multibody model of the CHARMIE robot has been developed utilizing the well-established Newton–Euler formulation and it is composed of 40 rigid bodies, interconnected by 34 revolute joints, ten prismatic joints, and three rigid joints.

Nature-inspired robots, which can be helpful in hazardous or confined environments, such as ruins and rubbles of collapsed buildings, nuclear power plants, pipelines, or surgical procedures, have also been developed within the framework of multibody dynamics [20]. Vossoughi et al. [21] proposed a new planar structure for a n-link snake-like robot to obtain passive motion by using springs in series with angular displacement actuators. The Gibbs–Appell formulation [22] was used to develop the dynamic equations of motion in a horizontal plane. This approach is quite interesting, not only because it allows permits the simplification in the dynamic equations but also it results in a very efficient solution in terms of the computational effort. The obtained results demonstrate that with the appropriate selection of initial conditions, joint angles operate in a limit cycle, allowing the robot to move steadily along a passive trajectory. Talaeizadeh et al. [23] also considered a snake-like robot model to compare the performance of a variant of the Kane's formulation with six different techniques based on the Lagrange's formulation. In order to assess the effectiveness of the mentioned methods, a snake-like robot was utilized, and several aspects, such as the number of the most time-consuming computational operations, constraint error, energy error, and CPU time allocated to each method were investigated. Saunders et al. [24] investigated the possibility of obtaining accurate optimal gait patterns for soft-body robots using a lumped dynamic model. These authors used a caterpillar-like soft robot to validate the approach. The problem of modeling and studying soft robots based on caterpillar locomotion was also object of investigation by Zou et al. [25], who developed a new robot capable of moving at 18.5 m/h. The modular structure of this robot is crucial to ensure a good ability to cope with the challenges of different environments and tasks. More recently, Jia and co-authors [26] proposed a new amphibious soft-rigid wheeled crawling robot that is composed by a soft-rigid body actuated by two soft pneumatic actuators, four wheels, and four annular soft bladders as brakes. The solution developed and built was very good in terms of locomotion performance in amphibious environment.

The modeling of the contact-impact phenomenon is one of the most important issues in the analysis of robotic systems. Many authors have recognized the critical role that the selection of the contact force model plays in the modeling and analysis of dynamical systems, and numerous normal and tangential contact force models have been extensively documented in the literature [27–33]. Contact conditions introduce complexities in the system that are effectively addressed through multibody dynamics simulations. These simulations allow researchers and engineers to study how robots respond to different terrains, forces, and environmental conditions. Two main steps must be considered in a contact problem in multibody dynamics, namely (*i*) the definition of the geometric properties of the surfaces in contact, together with the development of a methodology to access whether contact is occurring, and (*ii*) the calculation of the contact forces resulting from the collision. The modeling of contact-impact events strongly depends on multiple factors, such as the geometry of the contacting surfaces, the local physical properties, and the numerical representation of the interaction between the contacting bodies [34, 35]. In robotics, three main types of contact-impact phenomena can be considered, namely, the contacts than can take place between the robot's feet and the ground, the contacts arising from joint's clearance, and the interaction between the robot and the surrounding environment. This last issue is particularly relevant for applications in which robots are required to navigate through dynamic, unstructured, and uneven environments [36–39].

Multibody dynamics methodologies have also been applied in the process of modeling and studying several robotic systems to deal with the contact-impact phenomenon. Varedi-Koulaei et al. [40] studied

https://doi.org/10.1017/S026357472400050X Published online by Cambridge University Press

the dynamic behavior of a 3RRR planar parallel manipulator consisting of an equilateral triangular platform connected to the base by three legs, each of them composed of two bodies and three revolute clearance joints. Regularized models, for both normal and tangential forces, were considered to compute the intra-joint contact-impact forces developed at the clearance joints. In particular, the classical Hertz contact approach, incorporated with a dissipative term, was utilized to determine the normal contact forces. In turn, a Coulomb's friction force model was used to evaluate the tangential forces due the friction effect. Guo and co-authors [41] analyzed the dynamic response of a rigid-flexible multibody approach together with joint clearance in a 5-DOF polishing robot. In this work, the authors provided the theoretical background to improve the motion accuracy and dynamic performance of this type of hybrid polishing robot. In turn, Tian et al. [42] developed an adaptive impedance control method for the pneumatic servo-polishing system of the robot to ensure a constant contact force control problem between the end tool of a 5 degrees of freedom hybrid optical mirror processing robot and a workpiece. The computational and experimental results demonstrated the effectiveness of the presented approach, both in terms of accuracy and adaptability. Zahedi et al. [43] proposed a direct and simple formulation to derive the multibody equations of motion for constrained robotic mechanisms with multiple closed loops, which was verified with an experimental study. Farhat et al. [44] presented a switch algorithm to solve the discontinuity problem associated with the Coulomb's friction force model, which results in stiff differential equations in the simulation process. The proposed algorithm was utilized to study a simple one degree-of-freedom oscillator, and a three degrees-of-freedom RPS parallel manipulator. Ahmadizadeh et al. [45] modeled the contact-impact phenomenon in a multibody system composed of four rigid links connected by revolute joints. Different normal contact force models have been evaluated in the dynamic response of the multibody system. These authors demonstrated that the system response includes both non-impact and impact scenarios, which eventually affect the computational resolution of the equations of motion due to the very short collisions.

The contact interaction between robot's feet and ground is a ubiquitous scenario in humanoid robots and legged locomotion systems. Understanding how feet make contact with and respond to diverse surfaces is essential for activities like walking, running, or maintaining stability [46, 47]. Mahapatra et al. [48] studied the contact events between the ground and the feet of a hexapod robot in different types of terrain to improve the gait energy consumption. In this work, the authors used regularized forces models to evaluate the normal and friction forces developed during the collision events. He and Ren [49] proposed a numerical framework of the limit cycle walking based on multibody dynamics methodologies, focusing specifically on the interaction between the feet and the ground. These authors used a planar model composed of five rigid bodies, namely, two legs, two feet and the torso, connected by revolute joints. Geometrically, the ground was considered to be a planar surface, and the feet were considered as spheres or a series of points. Liu et al. [50] modeled and studied the dynamics of passive biped robot in terms of gait bifurcation, intermittency and crisis, which allows for designing controllers with less stringent torque requirements on biped walking robots. Tang and co-authors [51] proposed a new method to deal with earth-contact mechanism's performance map based on the digital terrain map, which helps the control system and operator to make the optimal control decision. The main benefits of the presented approach were examined with experiments.

The concept of contact joint was introduced by Hu and Guo [52] to model the foot–environment contact in challenging environments where the terrain may be composed of uneven and slippery surfaces. The authors validated their approach using a hexapod robot, with each leg consisting of a 2-UPS/UP parallel mechanism and a flat foot connected by a spherical joint. The proposed concept of a contact joint characterized the permissible foot motion, taking into account the geometric interactions between the foot and the environment. Tang et al. [53] presented a new knee exoskeleton with remote-center-of-motion mechanism with the purpose to improve the kinematic synergy between the exoskeleton and the human body. The authors proved the accuracy and applicability of their solution with data obtained from an experimental apparatus, being suggested the new design guidelines can be considered to better investigate exoskeleton robots for biomechanics human gait performance. David and Bruneau [54] presented a method, named sequential method of analytical potential, to generate dynamic walking gaits for bipedal

https://doi.org/10.1017/S026357472400050X Published online by Cambridge University Press

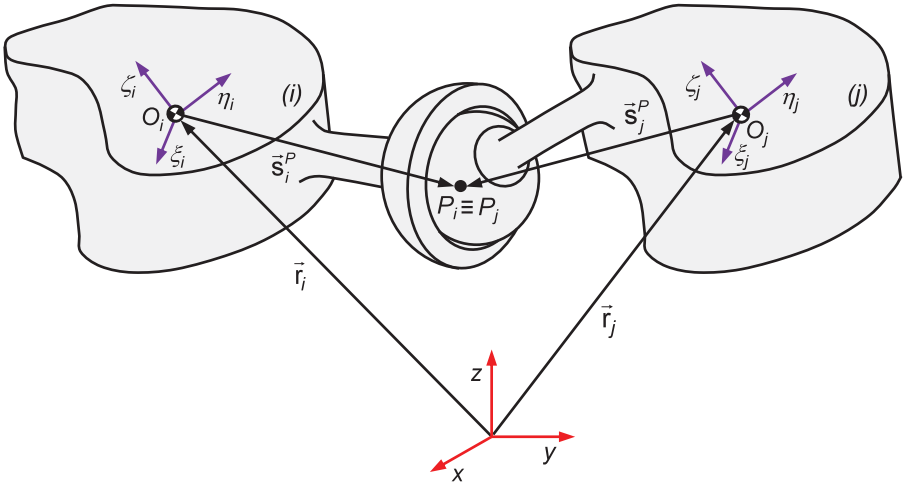

Figure 1. *Representation of a spherical joint linking two generic bodies i and j.*

robots. In this investigation, the authors used the Lagrange's formulation to develop a multibody model of the bipedal robot Rabbit and considered a single-point contact at the leg. The proposed approach had the advantage to be a unified framework, encompassing both the dynamics in the operational space and the system's instantaneous capabilities and limits, enabling a comprehensive understanding of the system's dynamic performance in the operational space [55].

2. Multibody formulations for robotics

2.1. Kinematic aspects of constraints in multibody systems

With the aim of formulating the equations of motion that govern the dynamic response of robotic systems, it is first necessary to elaborate on the key aspects related to their kinematic structures. By and large, the two main spatial joints utilized to model robotic systems are the spherical and revolute joints, which are briefly described in the following paragraphs. For a more in-depth exploration of multibody systems formulations, interested readers are directed to the work authored by Nikravesh [56].

Fig. 1 illustrates a typical spherical joint, commonly referred to as a ball-and-socket joint. This particular kinematic pair restricts the relative translations between the two adjacent bodies, denoted as i and j, while allowing for three relative rotations. Thus, the center of the spherical joint has constant coordinates with respect to any of the local coordinate systems of the connected bodies. In other words, a spherical joint establishes that the point P_i on body i shares the same position as the point P_j on body j. The kinematic constraints associated with a spherical joint can be written as [56–58]

$$\mathbf{\Phi}^{(s,3)} \equiv \mathbf{r}_j^P - \mathbf{r}_i^P = \mathbf{r}_j + \mathbf{s}_j^P - \mathbf{r}_i - \mathbf{s}_i^P = \mathbf{0} \tag{1}$$

in which, $\mathbf{r}$ and $\mathbf{s}$ denote the position vectors with respect to the global coordinate system xyz. The three scalar constraint equations implied by Eq. (1) restrict the relative position of points P_i and P_j. Thus, there are three degrees of freedom between two bodies connected by a spherical joint. The contributions to the Jacobian matrix ($\mathbf{J}$) of the constraints and to the right-hand side (γ) of the acceleration constraint equations can be derived conventionally, leading to the following expressions [56],

$$\mathbf{D}_{(3\times12)}^{(s,3)} = \begin{bmatrix} -\mathbf{I} & \tilde{\mathbf{s}}_i^P & \mathbf{I} & -\tilde{\mathbf{s}}_j^P \end{bmatrix} \tag{2}$$

$$\boldsymbol{\gamma}^{(s,3)} = -\dot{\tilde{\mathbf{s}}}_i^P \boldsymbol{\omega}_i + \dot{\tilde{\mathbf{s}}}_j^P \boldsymbol{\omega}_j \tag{3}$$

where $\mathbf{I}$ is the 3×3 identity matrix, $(\sim)$ represents the skew-symmetric vector, $(\cdot)$ is the first derivative with respect to time, and $\boldsymbol{\omega}$ denotes the angular velocity vector [58].

https://doi.org/10.1017/S026357472400050X Published online by Cambridge University Press

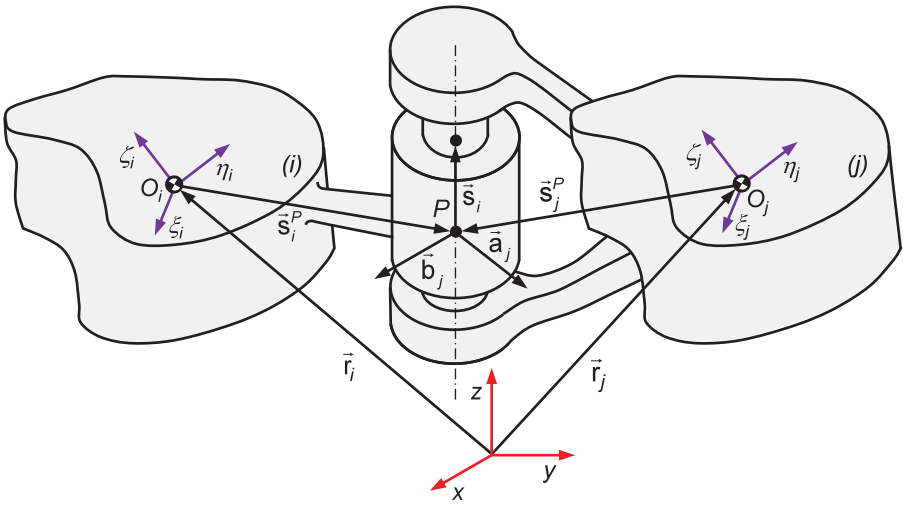

Figure 2. *Representation of a revolute joint linking two generic bodies i and j.*

A typical revolute joint, linking two generic bodies i and j, consists of a journal and a bearing. It allows a relative rotation about a common axis while preventing relative translation along this axis. Thus, Eq. (1) is imposed on an arbitrary point p located on the joint axis. Let us consider two vectors $\mathbf{a}_j$ and $\mathbf{b}_j$ on body j perpendicular to each other and perpendicular to the joint axis, as illustrated in the representation of Fig. 2. It is clear that these two vectors must remain perpendicular to vector $\mathbf{s}_i$ defined along the joint axis. Therefore, five constraint equations for a revolute joint can be expressed as [56]

$$\boldsymbol{\Phi}^{(r,5)} \equiv \begin{cases} \boldsymbol{\Phi}^{(s,3)} \equiv \mathbf{r}_j + \mathbf{s}_j^P - \mathbf{r}_i - \mathbf{s}_i^P = \mathbf{0} \\ \Phi^{(n1,1)} \equiv \mathbf{s}_i^{\mathrm{T}} \mathbf{a}_j = 0 \\ \Phi^{(n1,1)} \equiv \mathbf{s}_i^{\mathrm{T}} \mathbf{b}_j = 0 \end{cases} \tag{4}$$

In turn, the contributions to the Jacobian matrix, $\mathbf{J}$, of the constraints and to the right-hand side, γ, of the acceleration constraint equations related to a revolute joint can be formulated as [56]

$$\mathbf{D}_{(5\times12)}^{(r,5)} = \begin{bmatrix} -\mathbf{I} & \tilde{\mathbf{s}}_i^P & \mathbf{I} & -\tilde{\mathbf{s}}_j^P \\ \mathbf{0} & -\mathbf{a}_j^{\mathrm{T}} \tilde{\mathbf{s}}_i & \mathbf{0} & -\mathbf{s}_i^{\mathrm{T}} \tilde{\mathbf{a}}_j \\ \mathbf{0} & -\mathbf{b}_j^{\mathrm{T}} \tilde{\mathbf{s}}_i & \mathbf{0} & -\mathbf{s}_i^{\mathrm{T}} \tilde{\mathbf{b}}_j \end{bmatrix} \tag{5}$$

$$\boldsymbol{\gamma}^{(r,5)} = \begin{cases} -\tilde{\tilde{\mathbf{s}}}_i^P \boldsymbol{\omega}_i + \tilde{\tilde{\mathbf{s}}}_j^P \boldsymbol{\omega}_j \\ -\mathbf{s}_i^{\mathrm{T}} \tilde{\boldsymbol{\omega}}_j \dot{\mathbf{a}}_j - \mathbf{a}_j^{\mathrm{T}} \tilde{\boldsymbol{\omega}}_i \dot{\mathbf{s}}_i - 2\dot{\mathbf{a}}_j^{\mathrm{T}} \dot{\mathbf{s}}_i \\ -\mathbf{s}_i^{\mathrm{T}} \tilde{\boldsymbol{\omega}}_j \dot{\mathbf{b}}_j - \mathbf{b}_j^{\mathrm{T}} \tilde{\boldsymbol{\omega}}_i \dot{\mathbf{s}}_i - 2\dot{\mathbf{b}}_j^{\mathrm{T}} \dot{\mathbf{s}}_i \end{cases} \tag{6}$$

The kinematic constraint equations for a generic multibody system can be represented as [59]

$$\boldsymbol{\Phi} \equiv \boldsymbol{\Phi}\,(\mathbf{q}) = \mathbf{0} \tag{7}$$

where $\mathbf{q}$ is the vector of body coordinates, and Φ is a function that describes the kinematic constraints.

The first time derivative of Eq. (7) yields the velocity constraints that provide relations between the velocity variables of a system. The velocity constraints can be expressed as

$$\dot{\boldsymbol{\Phi}} \equiv \mathbf{D}\mathbf{v} = \mathbf{0} \tag{8}$$

https://doi.org/10.1017/S026357472400050X Published online by Cambridge University Press

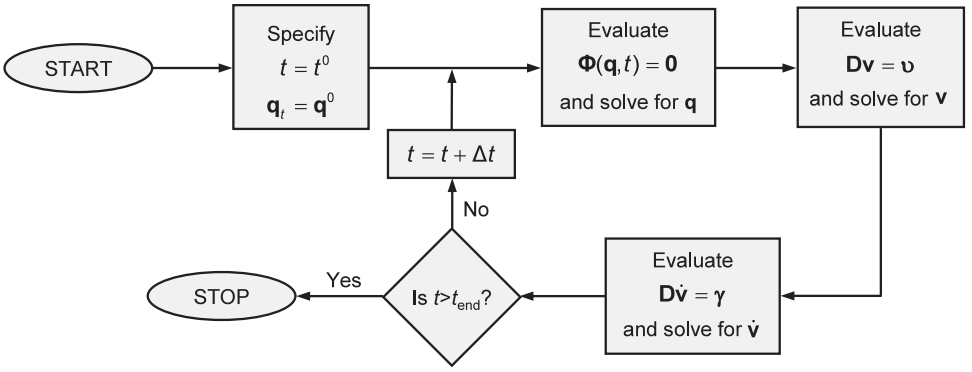

Figure 3. *Flowchart of computational procedure for kinematic analysis of multibody systems.*

in which $\mathbf{D}$ denotes the Jacobian matrix and $\mathbf{v}$ contains the velocity terms. For driving elements, the corresponding velocity constraint equations can be written in the form [56]

$$\dot{\mathbf{\Phi}} \equiv \mathbf{D}\mathbf{v} = \boldsymbol{\upsilon} \tag{9}$$

where the right-hand side contains the partial derivatives of Φ with respect to time, $\partial\Phi/\partial t$. The constraints at the velocity level are formulated as linear algebraic equations

The second time derivative of Eq. (7) results in

$$\ddot{\mathbf{\Phi}} \equiv \mathbf{D}\dot{\mathbf{v}} + \dot{\mathbf{D}}\mathbf{v} = \mathbf{0} \tag{10}$$

in which $\dot{\mathbf{v}}$ represents the acceleration terms, and the term $-\dot{\mathbf{D}}\mathbf{v}$ is the right-hand side of the kinematic acceleration equations. By defining $\boldsymbol{\gamma} = -\dot{\mathbf{D}}\mathbf{v}$, then, Eq. (9) can be rewritten

$$\mathbf{D}\dot{\mathbf{v}} = \boldsymbol{\gamma} \tag{11}$$

In should be noticed that the terms involved in Eqs. (7) through (11) appear in a general form, that is, they do not reflect the type of coordinates considered. The constraint equations represented by Eq. (7) are nonlinear in terms of $\mathbf{q}$ and can be solved by employing the Newton–Raphson method. Equations (8) and (11) are linear in terms of $\mathbf{v}$ and $\dot{\mathbf{v}}$, respectively, and can be solved by any standard method commonly employed for solving systems of linear equations. The kinematic analysis of a multibody systems can be carried out by solving Eqs. (7)-(11) together with the necessary driver constraints [56]. Thus, the necessary steps to perform this type of analysis, sketched in Fig. 3, are summarized as

1. Specify initial conditions for positions $\mathbf{q}^0$ and initialize the time t^0.
2. Compute the position constraint equations (7) and solve them for positions, $\mathbf{q}$.
3. Compute the velocity constraint equations (9) and solve them for velocities, $\mathbf{v}$.
4. Compute the acceleration constraint equations (11) and solve them for accelerations, $\dot{\mathbf{v}}$.
5. Increment the time. If the time is smaller than final time, go to step 2), otherwise stop the kinematic analysis.

2.2. Equations of motion for constrained multibody systems

The translational equations of motion for an unconstrained rigid body can be expressed as [56]

$$m\ddot{\mathbf{r}} = \mathbf{f} \tag{12}$$

where m denotes the mass of the body, $\ddot{\mathbf{r}}$ is the acceleration of the center of mass, and $\mathbf{f}$ represents the sum of all forces acting on the body. Nikravesh [56] demonstrated that the rotational equations of motion for a rigid body can be expressed in the form

$$\mathbf{J}\dot{\boldsymbol{\omega}} + \tilde{\boldsymbol{\omega}}\mathbf{J}\boldsymbol{\omega} = \mathbf{n} \tag{13}$$

https://doi.org/10.1017/S026357472400050X Published online by Cambridge University Press

in which $\mathbf{J}$ is the global inertia tensor, $\dot{\boldsymbol{\omega}}$ denotes the global angular accelerations, $\boldsymbol{\omega}$ is the global angular velocities, and $\mathbf{n}$ denotes the sum of all moments acting on the body. Thus, the translational and rotational equations of motion, commonly referred to as the Newton–Euler equations of motion, for an unconstrained body can be obtained by combining Eq. (12) and Eq. (13), which in the matrix form are written as [56]

$$\begin{bmatrix} m\mathbf{I} & \mathbf{0} \\ \mathbf{0} & \mathbf{J} \end{bmatrix} \begin{Bmatrix} \ddot{\mathbf{r}} \\ \dot{\boldsymbol{\omega}} \end{Bmatrix} = \begin{Bmatrix} \mathbf{f} \\ \mathbf{n} - \tilde{\boldsymbol{\omega}}\mathbf{J}\boldsymbol{\omega} \end{Bmatrix} \tag{14}$$

The equations of motion can also be derived and expressed in terms of local components, namely the rotational equations of motion. However, the form how the equations of motion are presented here is consistent with the kinematic constraints offered in the previous sections. Hence, in a compact form, Eq. (14) can be expressed as

$$\mathbf{M}_i \dot{\mathbf{v}}_i = \mathbf{g}_i \tag{15}$$

where

$$\mathbf{M}_i = \begin{bmatrix} m_i\mathbf{I} & \mathbf{0} \\ \mathbf{0} & \mathbf{J}_i \end{bmatrix}, \dot{\mathbf{v}}_i = \begin{Bmatrix} \ddot{\mathbf{r}}_i \\ \dot{\boldsymbol{\omega}}_i \end{Bmatrix}, \mathbf{g}_i = \begin{Bmatrix} \mathbf{f}_i \\ \mathbf{n}_i - \tilde{\boldsymbol{\omega}}_i\mathbf{J}_i\boldsymbol{\omega}_i \end{Bmatrix} \tag{16}$$

Hence, the Newton–Euler equations of motion of a multibody system composed by n_b unconstrained bodies are written as [56]

$$\mathbf{M}\dot{\mathbf{v}} = \mathbf{g} \tag{17}$$

For a multibody constrained system, the Newton–Euler equations of motion are written as

$$\mathbf{M}\dot{\mathbf{v}} = \mathbf{g} + \mathbf{g}^{(c)} \tag{18}$$

where $\mathbf{g}^{(c)}$ denotes the vector of reaction forces that can be expressed in terms of the Jacobian matrix and Lagrange multipliers as [60],

$$\mathbf{g}^{(c)} = \mathbf{D}^{\mathrm{T}}\boldsymbol{\lambda} \tag{19}$$

Finally, the equations of motion for a constrained multibody system can be written in its general form as

$$\mathbf{M}\dot{\mathbf{v}} - \mathbf{D}^{\mathrm{T}}\boldsymbol{\lambda} = \mathbf{g} \tag{20}$$

In dynamic analysis, a unique solution is obtained when the algebraic constraint equations at the acceleration level are considered simultaneously with the differential equations of motion. Therefore, the second time derivative of the constraint equations are considered here and written as [56]

$$\mathbf{D}\dot{\mathbf{v}} = \boldsymbol{\gamma} \tag{21}$$

Equation (21) can be appended to Eq. (20), resulting in a system of differential-algebraic equations (DAE) This system of equations is solved for accelerations vector, $\dot{\mathbf{v}}$, and Lagrange multipliers, λ. Then, in each integration time step, the accelerations vector, $\dot{\mathbf{v}}$, together with velocities vector, $\mathbf{v}$, is integrated in order to obtain the system velocities and positions for the next time step. This procedure is repeated until the final analysis time is reached. A set of initial conditions for positions and velocities is required to start the dynamic simulation. Often, the initial conditions are based on the results of kinematic analysis of the mechanical systems. The subsequent initial conditions for each time step in the simulation are obtained in the usual manner from the final conditions of the previous time step [61]. Thus, Eqs. (20) and (21) can be rewritten in the matrix form as

$$\begin{bmatrix} \mathbf{M} & \mathbf{D}^{\mathrm{T}} \\ \mathbf{D} & \mathbf{0} \end{bmatrix} \begin{Bmatrix} \dot{\mathbf{v}} \\ \boldsymbol{\lambda} \end{Bmatrix} = \begin{Bmatrix} \mathbf{g} \\ \boldsymbol{\gamma} \end{Bmatrix} \tag{22}$$

https://doi.org/10.1017/S026357472400050X Published online by Cambridge University Press

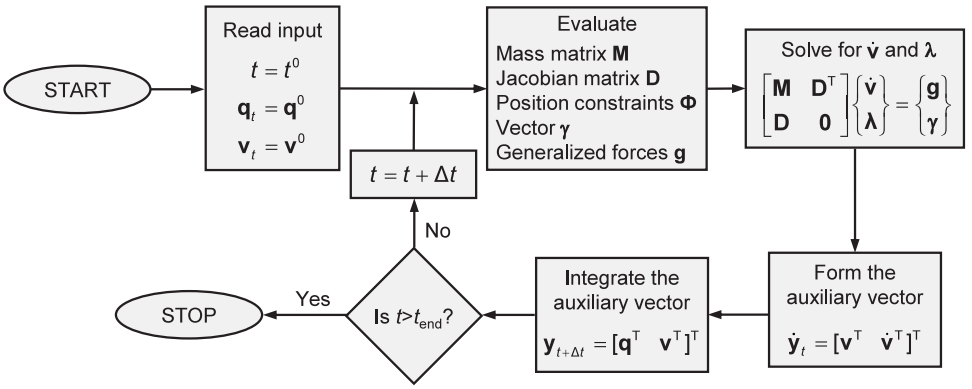

Figure 4. *Flowchart of computational procedure for dynamic analysis of multibody systems.*

The linear system of equations (22) can be solved by using any method suitable for the solution of linear algebraic equations. The existence of null elements in the main diagonal of the matrix and the possibility of ill-conditioned matrices suggest that methods using partial or full pivoting are preferred [62]. However, none of these formulations are effective in handling redundant constraints. For this purpose, Eq. (20) is rearranged to put the accelerations vector in evidence, yielding [63]

$$\dot{\mathbf{v}} = \mathbf{M}^{-1}\left(\mathbf{g} + \mathbf{D}^{\mathrm{T}}\boldsymbol{\lambda}\right) \tag{23}$$

In this process, it is assumed that the multibody system under analysis does not include any body with null mass or inertia, ensuring the existence of the inverse of the mass matrix **M**. Thus, introducing Eq. (23) into Eq. (21) and after basic mathematical manipulation results in

$$\boldsymbol{\lambda} = \left[\mathbf{D}\mathbf{M}^{-1}\mathbf{D}^{\mathrm{T}}\right]^{-1}\left(\boldsymbol{\gamma} - \mathbf{D}\mathbf{M}^{-1}\mathbf{g}\right) \tag{24}$$

Substituting now Eq. (24) into Eq. (23) yields

$$\dot{\mathbf{v}} = \mathbf{M}^{-1}\mathbf{g} + \mathbf{M}^{-1}\mathbf{D}^{\mathrm{T}}\left\{\left[\mathbf{D}\mathbf{M}^{-1}\mathbf{D}^{\mathrm{T}}\right]^{-1}\left(\boldsymbol{\gamma} - \mathbf{D}\mathbf{M}^{-1}\mathbf{g}\right)\right\} \tag{25}$$

Equation (25) can be solved for $\dot{\mathbf{v}}$ and, subsequently, the velocities and positions can be obtained through the integration process in a manner similar to the description provided above. This method for solving the dynamic equations of motion is commonly referred to as the standard Lagrange multipliers method [64]. Fig. 4 shows a flowchart depicting the algorithm for the standard solution of the equations of motion. At $t{=}t^0$, the initial conditions on $\mathbf{q}^0$ and $\mathbf{v}^0$ are required to start the integration process. These values cannot be specified arbitrarily, but must satisfy the constraint equations defined by Eqs. (7) and (8). The algorithm presented in Fig. 4 can be summarized by the following steps:

1. Start at instant of time t^0 with given initial conditions for positions $\mathbf{q}^0$ and velocities $\mathbf{v}^0$.
2. Assemble the global mass matrix **M**, evaluate the Jacobian matrix **D**, construct the constraint equations Φ, determine the right-hand side of the accelerations γ, and calculate the force vector **g**.
3. Solve the linear set of the equations of motion (23) for a constrained multibody system in order to obtain the accelerations $\dot{\mathbf{v}}$ at instant t and the Lagrange multipliers λ.
4. Assemble the vector $\dot{\mathbf{y}}_t$ containing the generalized velocities **v** and accelerations $\dot{\mathbf{v}}$ for instant t.
5. Integrate numerically the **v** and $\dot{\mathbf{v}}$ vectors for time step $t{+}\Delta t$ and obtain the new positions and velocities.
6. Update the time variable, go to step 2) and proceed with the process for a new time step, until the final time of analysis is reached.

https://doi.org/10.1017/S026357472400050X Published online by Cambridge University Press

The system of equations of motion (22) does not explicitly incorporate the position and velocity equations associated with the kinematic constraints, that is, Eqs. (7) and (8). Consequently, for moderate or long-time simulations, the original constraint equations may be violated due to the integration process and/or inaccurate initial conditions. Therefore, it is essential to implement methods capable of either eliminating errors in the position or velocity equations or, at a minimum, keeping such errors under control. In order to keep the constraint violations under control, the Baumgarte stabilization method is considered here [65–69]. This method permits constraints to be marginally violated before corrective actions are taken, in order to force the violation to vanish.

The objective of Baumgarte stabilization method is to replace the differential Eq. (10) by the following formulation [65]

$$\ddot{\mathbf{\Phi}} + 2\alpha\dot{\mathbf{\Phi}} + \beta^2\mathbf{\Phi} = \mathbf{0} \tag{26}$$

Equation (26) represents a differential equation for a closed-loop system in terms of kinematic constraint equations, in which the terms $2\alpha\dot{\mathbf{\Phi}}$ and $\beta^2\mathbf{\Phi}$ play the role of control terms. The principle of the method is based on the damping of acceleration of constraint violation by providing feedback on the position and velocity of constraint violations [63], which shows open-loop and closed-loop control systems. In the open-loop systems, $\mathbf{\Phi}$ and $\dot{\mathbf{\Phi}}$ do not converge to zero if any perturbation occurs and, therefore, the system is unstable. Thus, using the Baumgarte approach, the equations of motion for a system subjected to constraints are stated in the following form

$$\begin{bmatrix} \mathbf{M} & \mathbf{D}^{\mathrm{T}} \\ \mathbf{D} & \mathbf{0} \end{bmatrix} \begin{Bmatrix} \dot{\mathbf{v}} \\ \boldsymbol{\lambda} \end{Bmatrix} = \begin{Bmatrix} \mathbf{g} \\ \boldsymbol{\gamma} - 2\alpha\dot{\mathbf{\Phi}} - \beta^2\mathbf{\Phi} \end{Bmatrix} \tag{27}$$

If α and β are chosen as positive constants, the stability of the general solution of Eq. (27) is guaranteed. Baumgarte [65] highlighted that the suitable choice of the parameters α and β is performed by numerical experiments. Hence, the Baumgarte method introduces some ambiguity in determining optimal feedback gains. The values of the parameters appear to be purely empirical, lacking a reliable method for selecting the coefficients α and β. The improper choice of these coefficients can lead to unacceptable results in the dynamic analysis of the multibody systems [70]. The coordinate partitioning method [71], the penalty approach [72], and the augmented Lagrangian formulation [73] are alternative methods for addressing the violation of constraints.

3. Contact interactions formulation

3.1. Contact kinematics

Contact kinematics deals with the determination of potential contact points, contact detection, and relative contact velocity [74–76]. In general, this information must be available in order to allow the evaluation of the contact forces developed during contact events. In order to better understand how these ingredients are computed in multibody dynamics, Let consider the scenario involving two rigid bodies that can potentially collide with each other, as illustrated in Fig. 5. In the situation depicted in Fig. 5a, two convex bodies i and j are in the state of separation and moving with absolute velocities $\dot{\mathbf{r}}_i$ and $\dot{\mathbf{r}}_j$, respectively.

The possible motion of each body within a multibody system can be quantified by assessing the distance and relative velocity of the potential contact points. Positive values of that distance represent a separation, while negative values denote relative pseudo-penetration, or indentation, of the colliding bodies. These two distinct situations are represented in Fig. 5a and 5b, respectively. The change in sign of the normal distance indicates a transition from separation to contact, or vice versa [77]. In turn, positive values of the relative normal velocity between the potential contact points, that is, the penetration or deformation velocity, indicate that the bodies are approaching, which corresponds to the compression phase, while negative values denote that the bodies are separating, that corresponds to the restitution

https://doi.org/10.1017/S026357472400050X Published online by Cambridge University Press

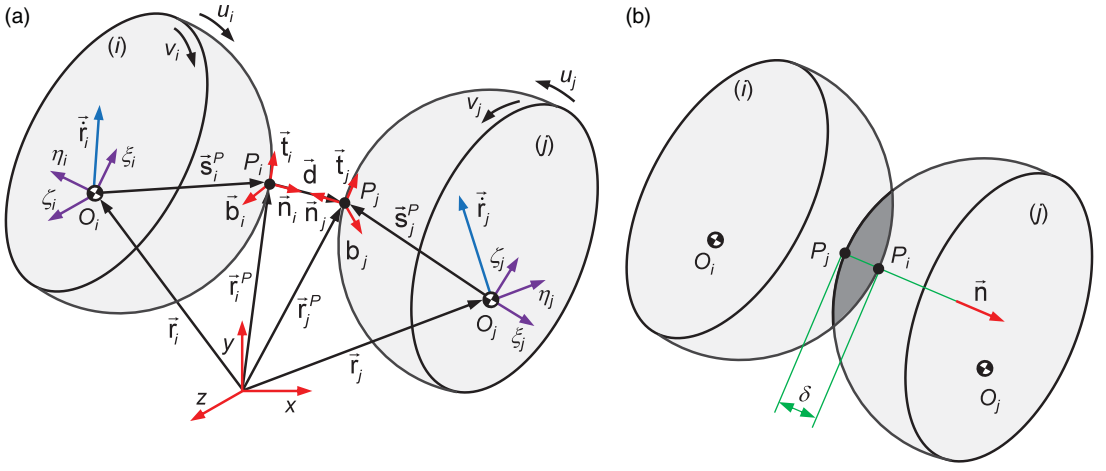

Figure 5. *(a) Two bodies in the state of separation; (b) Two bodies in the state of contact.*

phase. [78] The fundamental kinematic vectors of interest when modeling and analyzing contact events in the context of multibody dynamics are depicted in Fig. 5 [79–81].

With regard to Fig. 5, the vector that connects the two potential contact points, P_i and P_j, is a gap function that can be written in the form [56]

$$\mathbf{d} = \mathbf{r}_j^P - \mathbf{r}_i^P \tag{28}$$

where vectors $\mathbf{r}_i^P$ and $\mathbf{r}_j^P$ are expressed in terms of global coordinates

$$\mathbf{r}_k^P = \mathbf{r}_k + \mathbf{A}_k \mathbf{s}_k'^P \quad (k = i, j) \tag{29}$$

in which $\mathbf{r}_i$ and $\mathbf{r}_j$ represent the global position vectors of the bodies i and j, while $\mathbf{s}_i'^P$ and $\mathbf{s}_j'^P$ denote the local components of the potential contact points with respect to local coordinates systems. In turn, $\mathbf{A}_i$ and $\mathbf{A}_j$ are the rotational transformation matrices of the bodies i and j, respectively [56].

The normal vector to the plane of contact of two surfaces, as represented in Fig. 5, can be expressed as

$$\mathbf{n} = \frac{\mathbf{d}}{d} \tag{30}$$

For a generic regular parametric surface defined by u-v mapping, the trihedral ($\mathbf{t}$, $\mathbf{b}$, $\mathbf{n}$) at point $\mathbf{s}(u, v)$ of the surfaces is obtained using the following formulation [74]

$$\mathbf{t} = \frac{\partial \mathbf{s}}{\partial u}, \quad \mathbf{b} = \frac{\partial \mathbf{s}}{\partial v}, \quad \mathbf{n} = \frac{\mathbf{t} \times \mathbf{b}}{|\mathbf{t} \times \mathbf{b}|} \tag{31}$$

in which (u, v) are arranged such that the vector $\mathbf{n}$ becomes the outward normal, as in Fig. 5 [82–84].

The magnitude of the distance vector $\mathbf{d}$, which represents a gap or penetration, can be evaluated as

$$d = \delta = \mathbf{d}^{\mathrm{T}} \mathbf{n} \tag{32}$$

while fulfilling the conditions that the distance vector is aligned with the normal vectors of the contacting surfaces, yielding [83]

$$\mathbf{d} \times \mathbf{n}_i = \mathbf{0} \Leftrightarrow \begin{cases} \mathbf{d}^{\mathrm{T}} \mathbf{t}_i = 0 \\ \mathbf{d}^{\mathrm{T}} \mathbf{b}_i = 0 \end{cases}, \qquad \mathbf{d} \times \mathbf{n}_j = \mathbf{0} \Leftrightarrow \begin{cases} \mathbf{d}^{\mathrm{T}} \mathbf{t}_j = 0 \\ \mathbf{d}^{\mathrm{T}} \mathbf{b}_j = 0 \end{cases} \tag{33}$$

where $\mathbf{t}_k$ and $\mathbf{b}_k$ (k=i, j) represent the tangential and binormal vectors illustrated in Fig. 5. It should be noted that the inner products between $\mathbf{d}$ and surfaces tangent and binormal vectors are equivalent to the cross products between $\mathbf{d}$ and the corresponding vectors normal to the surfaces [83]. At this stage, it is

https://doi.org/10.1017/S026357472400050X Published online by Cambridge University Press

important to mention that P_i and P_j are the contact points when the surfaces normal vectors $\mathbf{n}_i$ and $\mathbf{n}_j$ are collinear with the distance vector $\mathbf{d}$. These conditions can be obtained by two cross products between vectors $\mathbf{d}$ and $\mathbf{n}_i$, and $\mathbf{d}$ and $\mathbf{n}_j$, and expressed by Eqs. (33). In fact, the geometric conditions given by Eqs. (33) constitute four nonlinear equations with four unknowns, which can be solved by utilizing an iterative numerical algorithm such as the Newton–Raphson method [56], providing the location of the candidate contact points [83]. Once the candidate contact points are determined, the subsequent step deals with the evaluating of their relative distance using Eq. (32). Then, it is required to verify the penetration condition, which ensures that the contact exists, that is, the candidate contact points are actual contact points [82–86]. Once the contact points are identified, the next step involves evaluating the relative penetration between the contact bodies [87].

The absolute velocities of the potential contact points can be expressed in terms of the global coordinate system by differentiating Eq. (29) with respect to time, yielding

$$\dot{\mathbf{r}}_k^P = \dot{\mathbf{r}}_k + \dot{\mathbf{A}}_k \mathbf{s}_k'^P \tag{34}$$

in which the dot denotes the derivative with respect to time. The scalar normal and tangential velocities can be determined using the following expression

$$v_{\mathrm{n}} = \dot{\delta} = \left(\dot{\mathbf{r}}_j^P - \dot{\mathbf{r}}_i^P\right)^{\mathrm{T}} \mathbf{n} \tag{35}$$

$$v_{\mathrm{t}} = \left(\dot{\mathbf{r}}_j^P - \dot{\mathbf{r}}_i^P\right)^{\mathrm{T}} \mathbf{t} \tag{36}$$

This representation of the relative normal and tangential velocities is quite convenient, in the measure that there is no need to deal with the derivation of the normal unit vector because the velocities components are not directly obtained by differentiating Eq. (32). Moreover, the fully rigid body velocity kinematics can easily be applied, and the computational implementation of this method is extremely efficient. However, this approach is limited to convex rigid bodies with smooth surfaces, at least in a neighborhood of the potential contact points. In this scenario, the contact area can be reduced to a single point that may move relative to the surfaces of the bodies. This approach can be extended to more generalized contact geometries as long as a common tangent plane of the contacting bodies is uniquely defined [83–90].

3.2. Contact resolution

In the context of multibody dynamics, resolving the contact involves the calculation of the normal and tangential forces developed at the contact, as well as the introduction of the resulting contact forces into the multibody system equations of motion of the system under analysis [91–98]. By and large, there are two main techniques to solve contact dynamic problems, namely, the regularized approaches (continuous methods) and the non-smooth formulations (piecewise methods) [99–101]. The former methods assume that the colliding bodies are deformable at the contact zone, allowing the contact forces to be expressed as a continuous function of the local deformation. Conversely, in non-smooth techniques, the contacting bodies are assumed to be perfectly rigid, and the contact dynamics is resolved by applying unilateral constraints in order to avoid the penetration from occurring [102–104].

Regularized approaches are quite popular in multibody dynamics due to their computational efficiency and straightforward implementation. Nevertheless, in some circumstances, numerical problems can arise due to poorly conditioned system matrices [105]. With regularized methods, there are no impulses involved in the impact process, and, therefore, there is no need for impulse dynamics computations. As a result, the transition between contact and non-contact situations can be easily handled through the system configuration and contact kinematics [78]. In these methods, the contact forces incorporate spring-damper elements to prevent interpenetration. In regularized approaches, the location of the contact point does not coincide in the contacting bodies, and there exists a large number of potential contact points, being the actual contact point is the one associated with the maximum deformation. The pseudo-penetration plays a key role as it is utilized to calculate the contact reaction forces according to

https://doi.org/10.1017/S026357472400050X Published online by Cambridge University Press

an appropriate constitutive law [92]. In general, contact force models can incorporate viscoelastic and plastic terms, along with considerations for contact kinematics and geometric properties of the contacting surfaces [106, 107]. The existence of friction in the continuous methods can easily be incorporated by considering any regularized friction force model [108–110].

A drawback associated with regularized approaches pertains to the estimation of contact parameters, especially when the contact geometry is complex in nature [111, 112]. A second difficulty of the regularized methods is the introduction of high-frequency dynamics into the system due to the existence of contact related spring-damper elements in the contacting surfaces. Therefore, when the dynamics requires the integration scheme to take small time steps, then the computational efficiency can be penalized. In methods based on non-smooth formulations, the contact points on both colliding bodies are necessarily coincident due to the unilateral constraints introduced into the system. In these methods, the relative interpenetration between the colliding bodies is not allowed, as the bodies are considered to be absolutely rigid at the contact zone [92, 113, 114].

Assuming that the contacting bodies are absolutely rigid, in contrast to locally deformable bodies as in regularized approaches, non-smooth formulations resolve contact-impact problems using unilateral constraints to determine impulses, preventing penetration from occurring. Fundamental to non-smooth methods is the explicit formulation of unilateral constraints between colliding rigid bodies [103, 115]. The core concept of non-smooth formulations lies in the non-penetration condition that only prevents bodies from moving toward each other and not apart, reason why this approach is called unilateral constraint [116, 117]. For this purpose, a complementarity formulation is employed to describe the relation between contact force and gap distance at the contact point. Such unilateral constraint does not permit the interpenetration of the two colliding bodies and ensures that either contact force or gap distance is null. This means that, when the gap distance is positive (open or inactive contact), the corresponding contact force is null. Conversely, when the contact force is positive (closed or active contact), the gap distance is null [102]. Thus, this formulation leads to a complementarity problem, serving as the framework that enables the treatment of multibody systems with unilateral constraints [118, 119].

The numerical issues associated with regularized approaches may not arise in non-smooth methods, but they introduce different challenges and requirements [120, 121]. For instance, the existence of a unique solution is not ensured, because in some cases, the system can be undetermined or have multiple solutions [122–124]. In general, commercial multibody codes equipped with collision and dry friction features handle the non-smooth nature of the problem through an ad hoc regularized approach. In fact, they use continuous models to prevent undesired interpenetration between bodies, which can ultimately lead to some numerical and computational difficulties.

Fig. 6 shows the graphical representation of the normal and tangential contact forces for the regularized approaches and non-smooth formulations. both the regularized approaches and the non-smooth methods employed to address contact-impact events within the framework of multibody dynamics have inherent advantages and disadvantages. Regardless, none of these briefly characterized techniques can be unequivocally identified as superior. A particular multibody system with collision events might easily be described by one method, nevertheless, this does not automatically imply a general predominance of that formulation in all multibody applications [125–128].

Table I lists the key characteristics associated with regularized and non-smooth methods, allowing for a comparative analysis. One critical issue related to frictional contact problems, affecting the accuracy and fidelity of the results obtained, pertains to the discretization or modeling process of the mechanical system under analysis. If the problem is well discretized, in general, both regularized and non-smooth techniques are effective in addressing frictional problems. In any case, the evaluation of the geometry of contact is the same, regardless of the chosen technique used to model the contact interaction between the colliding bodies, whether it be regularized approaches or non-smooth formulations [129, 130].

Contact mechanics in multibody systems deals with the modeling and analysis of deformation of solid parts when they contact or collision with each other. The specific case of frictional contact mechanics involves the analysis of collisions that include frictional phenomena [131]. It is noteworthy that contact mechanics plays a ubiquitous role in many multibody systems applications, and in most of the cases,

https://doi.org/10.1017/S026357472400050X Published online by Cambridge University Press

Table I. *Comparison between regularized and non-smooth methods to deal with contact problems.*

Regularized approaches	**Non-smooth formulations**
Bodies can locally deform	Bodies are strictly rigid
Pseudo-penetration is allowed	Impenetrability condition is utilized
Contact forces are continuous	Impulse-momentum is applied
Can cause high-frequency	Are robust and stable
Small time steps are required	Large time steps can be used
Local properties can be difficult to establish	Local properties are simple to identify
Multiple contacts are easy to handle	Difficult for multiple contacts
Differential equations are stiff	Undetermined and multiple solution can arise
Easy to implement	Not easy to generalize

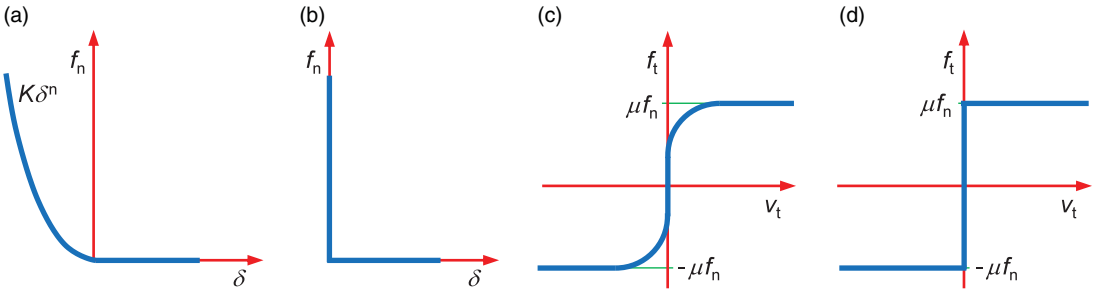

Figure 6. *(a) Regularized normal contact force model; (b) Non-smooth normal contact force model; (c) Regularized tangential contact force model; (d) Non-smooth tangential contact force model.*

their behavior and performance are strongly affected by the modeling process for contact-impact events [132–134]. Contact dynamics, focused on analyzing the motion of multibody systems experiencing collisions, remains one of the most challenging domains in both science and engineering [135–141].

The subject of contact mechanics and its applications in multibody dynamics had not been developed until the past few decades. Wittenberg [142], Wehage [143], and Khulief et al. [144] utilized a piecewise approach to handle impact events in multibody systems. In this discontinuous technique, the resolution of the equations of motion is halted at the instant of collision, where an impulse-momentum balance is performed to obtain the rebound velocities. The resolution of the equations of motion is then resumed with the updated velocities until a new collision takes place. Wehage and Haug [145] utilized the Newton's impact law together with piecewise contact approach to discuss contact problems in constrained multibody mechanical systems. Khulief and Shabana [146] formulated the generalized impulse-momentum balance equations to analyze impacts in multibody systems.

The problem of friction in multibody dynamics was investigated by Khulief [147]. Battle and Condomines [148] utilized a Lagrangian formulation and impulsive drivers to maintain the continuity of a set of generalized velocities during the impact process to model collisions in dynamical systems. A similar analysis was conducted by Lankarani and Nikravesh [149] to treat multibody systems with intermittent motion. These authors demonstrated that the numerical resolution of the canonical equations of motion is quite efficient and stable. Haug et al. [150] formulated and solved the equations of motion using the Lagrange multipliers technique. The Newton's hypothesis and Coulomb's friction law were considered to represent the impacts. The problem was replicated by Wang and Kumar [151] and Anitescu et al. [152], solution of which was obtained as a quadratic programing problem.

Over the past decades, the multibody dynamics community has exhibited an increasing interest in the resolution of the problems related to collisions between mechanical components. Actual examples of multibody mechanical systems in which contact–impact interactions play a crucial role are grasping and fingers contacts [153–157], robotics and walking machines [158–161], vehicle and railway subsystems

https://doi.org/10.1017/S026357472400050X Published online by Cambridge University Press

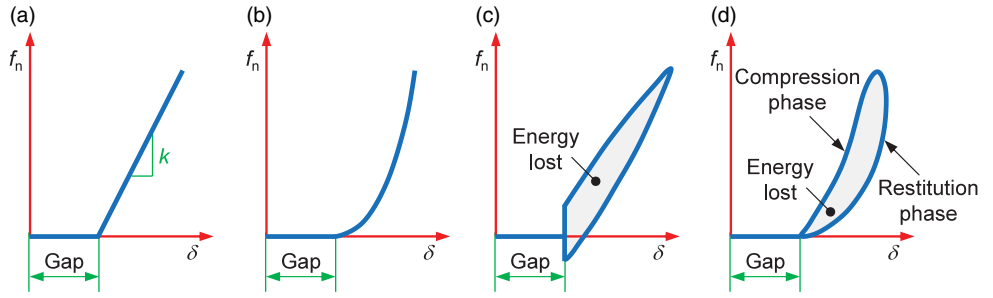

Figure 7. *Force-penetration relations for different contact force models: (a) Hooke's law; (b) Hertz's law; (c) Kelvin-Voigt approach; (d) Hunt and Crossley contact force model. The gap illustrated in these representations is the distance when the potential contact bodies are in a separation status.*

[162–171], biosystems and biomechatronics [172–178], machines and mechanisms [179–187], granular media and powder technologies [188–192], toys models [193–201], civil structures [202–211], sounds and musical instruments [212–217], and fruit transport and handling [218–223], just to mention some examples under the umbrella of dynamical systems.

The topic of contact-impact problems in dynamical systems has received a great deal of attention in the past decades and still remains an active area of research that led to the establishment of important works and even the publication of relevant textbooks devoted to this theme, such as the ones by Pfeiffer and Glocker [102], Glocker [224], Leine and Nijmeijer [225], Pfeiffer [226], Acary and Brogliato [227], and Flores and Lankarani [228]. Additionally, the interested reader is also referred to the following seminal works on contact problems [76, 93, 114, 229–231].

Finally, challenges and future directions for research under the framework of contact mechanics in multibody dynamics may include: the identification and estimation of the contact parameters for complex scenarios; the development of benchmark problems to assess the suitability of the existing techniques to handle contact-impact events; the analysis of contact problems with very large contact areas; the study of contacts with very flexible bodies; and the development of techniques to accelerate the contact detection with multiple potential contacts.

4. Continuous contact force models

4.1. Normal force models

The simplest contact force model is associated with Hooke's theory, and it can be applied when contact is active. This regularized force model incorporates a linear spring to mimic the contact interaction and can be written as [232]

$$f_n = k\delta \tag{37}$$

in which k represents the spring stiffness related to the contact materials, and δ denotes the penetration between the contacting surfaces (32). Fig. 7a shows the representation of the plot force–penetration for the Hooke contact force model. This approach is quite simple, but does not account for any kind of energy dissipation during the contact process.

A superior contact force model was formulated by Hertz, introducing a nonlinear relation between force and penetration [233]

$$f_n = K\delta^n \tag{38}$$

where the nonlinear exponent, n, is typically equal to 3/2. Fig. 7b depicts the force–penetration relation for the nonlinear Hertz's law. The Hertz contact force model is incapable of predicting any energy dissipation associated with contact-impact events. The value of the contact stiffness parameter, K, can be evaluated analytically as function of the material and geometric properties of the contacting surfaces.

https://doi.org/10.1017/S026357472400050X Published online by Cambridge University Press

Thus, based on the Hertz contact theory, the contact stiffness for two solid and isotropic spheres in contact can be established as

$$K = \frac{4}{3\left(\sigma_i + \sigma_j\right)}\sqrt{\frac{R_i R_j}{R_i + R_j}} \tag{39}$$

where the material properties, σ_1 and σ_2, are defined as

$$\sigma_k = \frac{1 - \nu_k^2}{E_k} \quad (k = i, j) \tag{40}$$

and the quantities ν_k and E_k are, respectively, the Poisson's ratio and Young's modulus of each sphere in contact. It should be noted that, by definition, the radius is positive for convex surfaces and negative for concave surfaces [63].

The first contact force model that accommodates energy dissipation in collisions is the Kelvin–Voigt approach, which combines a linear spring with a linear damper to represent the contact forces as [234]

$$f_{\mathrm{n}} = K\delta + D\dot{\delta} \tag{41}$$

where the first parcel denotes the elastic force term, and the second parcel denotes the dissipative force component, in which D represents the damping coefficient, and $\dot{\delta}$ is the normal relative velocity of the contacting bodies (35). Fig. 7c illustrates the force–penetration relation for the linear Kelvin–Voigt contact force model. It is important to mention that this approach displays discontinuities at the initiation and termination of the contact process. Indeed, the damping term introduces finite forces when the penetration is zero, which is not acceptable from a physical point of view. Furthermore, at the end of contact, the Kelvin–Voigt force model produces negative forces, which are not physically correct, as bodies involved in a collision cannot attract each other.

Hunt and Crossley proposed a contact force model that incorporates a nonlinear spring and a nonlinear damper in parallel to simulate the contact interaction. This force model can be formulated as [235]

$$f_{\mathrm{n}} = K\delta^n\left[1 + \frac{3\left(1 - c_{\mathrm{r}}\right)}{2}\frac{\dot{\delta}}{\dot{\delta}^{(-)}}\right] \tag{42}$$

where the first term represents the nonlinear elastic Hertz's law, and the second term is the dissipative parcel, being c_{r} the coefficient of restitution, and $\dot{\delta}^{(-)}$ is the normal contact velocity at the initial instant of impact. Fig. 7d illustrates the force–penetration evolution for the Hunt and Crossley contact force model, revealing the compression and restitution phases of an impact. In this diagram, the area of the hysteresis loop represents the amount of energy lost during the impact process. The Hunt and Crossley force model does not exhibit any discontinuity at the beginning or ending of the collision.

The most widely used contact force model in multibody dynamics is the one proposed by Lankarani and Nikravesh [53]. It was developed based on the Hertzian theory and incorporates the damping approach by Hunt and Crossley. Lankarani and Nikravesh contact force model can be expressed as

$$f_{\mathrm{n}} = K\delta^n\left[1 + \frac{3\left(1 - c_{\mathrm{r}}^2\right)}{4}\frac{\dot{\delta}}{\dot{\delta}^{(-)}}\right] \tag{43}$$

This model is valid for collisions with high values of the coefficient of restitution, making it applicable to elastic impacts. The contact force model presented by Lankarani and Nikravesh has been utilized in many areas of science and engineering.

Flores et al. [92] presented a contact force model that is applicable to the entire range of possible values for the coefficient of restitution, which is given by

$$f_{\mathrm{n}} = K\delta^n\left[1 + \frac{8\left(1 - c_{\mathrm{r}}\right)}{5c_{\mathrm{r}}}\frac{\dot{\delta}}{\dot{\delta}^{(-)}}\right] \tag{44}$$

https://doi.org/10.1017/S026357472400050X Published online by Cambridge University Press

he use of the contact force models (43) and (44) results in a similar evolution of the force–penetration diagram as in the case of the Hunt and Crossley approach (see Fig. 7d). For low values of the coefficient of restitution, the hysteresis loop for the Flores et al. contact force model is larger. It must be noticed that the force models (42)-(44) can exhibit some limitations when the contacts are too long, and when the velocity ratio $\dot{\delta}/\dot{\delta}^{(-)}$ becomes significantly less than –1 [236, 237]. Over the past few years, a significant number of contact force models have been presented in the literature. For detailed information, the interested reader is referred to the following references [238–240].

4.2. Friction force models

Friction is the interaction between two objects as one rubs against the other. In other words, friction is the resistance an object experiences when moving over another. In fact, when two contacting bodies move or tend to move relative to each other, tangential forces are developed at the surfaces of interaction. In multibody dynamics, the presence of friction on contact surfaces complicates and adds complexity to contact problems. Friction introduces different contact behaviors, encompassing both sticking and sliding. Stiction, occurring when the relative tangential velocity between two contacting surfaces approaches zero, is a phenomenon that the friction model employed in dynamic analysis must accurately predict [241].

Da Vinci was a pioneer in the study of friction, particularly in terms of the required weight needed to be applied to different objects placed on horizontal and inclined planes to initiate their motion [242]. Based on experimental observations, da Vinci formulated two fundamental laws of friction. The first law states that the friction generated by the same weight will exhibit equal resistance at the beginning of its movement, even if the contact area varies in width and length. The second law of friction posits that friction produces twice the effect when the weight is doubled. Amontons developed his experimental apparatus to investigate friction and rediscovered the laws of friction formulated by da Vinci [243]. According to Amontons, the friction law can be expressed as: (*i*) the friction force is independent of the apparent area of contact between the two surfaces in contact and (*ii*) the force of friction acting between two sliding surfaces is proportional to the load pressing the surfaces. Coulomb, arguably the most renowned name in the field of friction, published laws of friction, referring to the work of Amontons [244]. Coulomb extended Amontons' friction laws to a modern conceptual framework, and these laws are still used today. The two basic Coulomb's friction laws can be stated as (*i*) the friction force is independent of the nominal area of contact and (*ii*) the friction is proportional to the normal contact force.

The dry Coulomb's friction law can be expressed as

$$f_t = \begin{cases} \left[-\mu_k f_n,\ \mu_k f_n\right] & \text{if } \|\mathbf{v}_t\| = 0 \\ \mu_k f_n \text{sgn}\,(\mathbf{v}_t) & \text{if } \|\mathbf{v}_t\| \neq 0 \end{cases} \tag{45}$$

where

$$\text{sgn}\,(\mathbf{v}_t) = \begin{cases} \dfrac{\mathbf{v}_t}{\|\mathbf{v}_t\|} & \text{if } \|\mathbf{v}_t\| \neq 0 \\ 0 & \text{if } \|\mathbf{v}_t\| = 0 \end{cases} \tag{46}$$

in which μ_k is the kinetic coefficient of friction, f_n is the normal contact force, and $\mathbf{v}_t$ is the tangential velocity vector. The first branch of Eq. (45) is referred to as static or stiction friction, while the second branch is named dynamic or sliding friction. Fig. 8a shows the representation of the Coulomb's friction force model. It is important to note that this friction law poses some numerical challenges in terms of computational implementation in multibody simulations when the tangential relative velocity is zero.

Threlfall [245] introduced a regularized friction force model that avoids discontinuities, as it is evident from the observation of diagram in Fig. 8b. The Threlfall friction force model can be written as

https://doi.org/10.1017/S026357472400050X Published online by Cambridge University Press

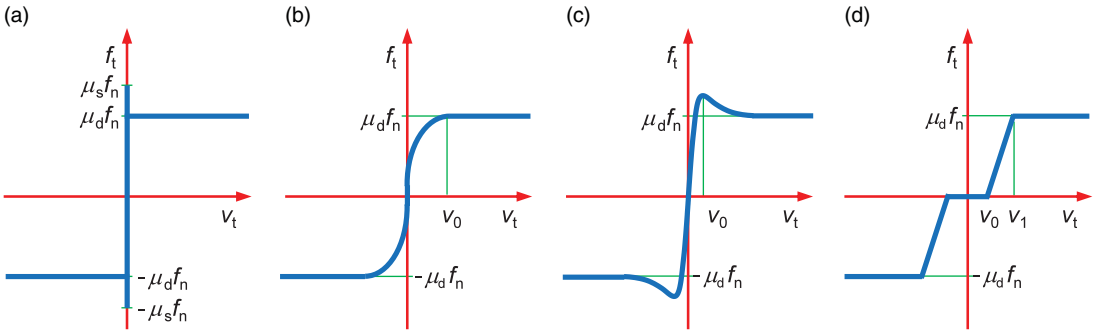

Figure 8. *Representation of several friction force models: (a) Coulomb's friction law; (b) Threlfall friction force model; (c) Bengisu and Akay friction force model; (d) Ambrósio friction force model.*

$$f_t = \begin{cases} \mu_k f_n \left(1 - e^{-3\frac{\|\mathbf{v}_t\|}{v_0}}\right) \operatorname{sgn}(\mathbf{v}_t) & \text{if } v_0 \leq \|\mathbf{v}_t\| \leq v_0 \\ 0.95\mu_k f_n \operatorname{sgn}(\mathbf{v}_t) & \text{if } \|\mathbf{v}_t\| > v_0 \end{cases} \tag{47}$$

in which v_0 represents the tolerance sliding velocity.

Bengisu and Akay [246] introduced a static friction model in order to capture the stiction behavior of friction. An enhanced version proposed by Marques et al. [30] is expressed by piecewise function as

$$f_t = \begin{cases} \left[-\frac{\mu_s f_n}{v_0^2}(\|\mathbf{v}_t\| - v_0)^2 + \mu_s f_n\right] \operatorname{sgn}(\mathbf{v}_t) & \text{if } \|\mathbf{v}_t\| < v_0 \\ \left[\mu_k f_n + (\mu_s f_n - \mu_k f_n)\, e^{-\xi(\|\mathbf{v}_t\| - v_0)}\right] \operatorname{sgn}(\mathbf{v}_t) & \text{if } \|\mathbf{v}_t\| \geq v_0 \end{cases} \tag{48}$$

where μ_s is the static friction coefficient and ξ is a positive parameter related to the negative slope of the sliding state associated with the Stribeck effect. Fig. 8c illustrates the evolution of the Bengisu and Akay friction force model.

Ambrósio [247] suggested another regularized approach for Coulomb's law, which incorporates a ramp to overcome numerical difficulties. This friction force model can be expressed as

$$f_t = c_d \mu_k f_n \operatorname{sgn}(\mathbf{v}_t) \tag{49}$$

with

$$c_d = \begin{cases} 0 & \text{if } \|\mathbf{v}_t\| < v_0 \\ \dfrac{\|\mathbf{v}_t\| - v_0}{v_1 - v_0} & \text{if } v_0 \leq \|\mathbf{v}_t\| \leq v_1 \\ 1 & \text{if } \|\mathbf{v}_t\| > v_1 \end{cases} \tag{50}$$

in which the dynamic correction factor, c_d, prevents the friction force from changing direction for almost null values of the tangential relative velocity. Fig. 8d shows Ambrósio's friction approach.

The utilization of the friction models (47), (48), and (49) offers the advantage of enabling the numerical stabilization of the integration algorithm used in resolving the equations of motion for constrained multibody systems. These approaches do not account for stiction. Therefore, several alternative friction force models have been proposed over the past few decades. Interested readers are referred to the following references for more detailed information [248–254].

Most of the aforementioned friction force models smooth Coulomb's law, making them continuous or regularized solutions. This characteristic enables a stable and efficient resolution of the equations of motion for multibody mechanical systems. It should be noted that a straightforward and clear rule of thumb for selecting appropriate values for the parameters involved in the described friction models is not readily available. Typically, their choice relies on the trial-and-error method.

https://doi.org/10.1017/S026357472400050X Published online by Cambridge University Press

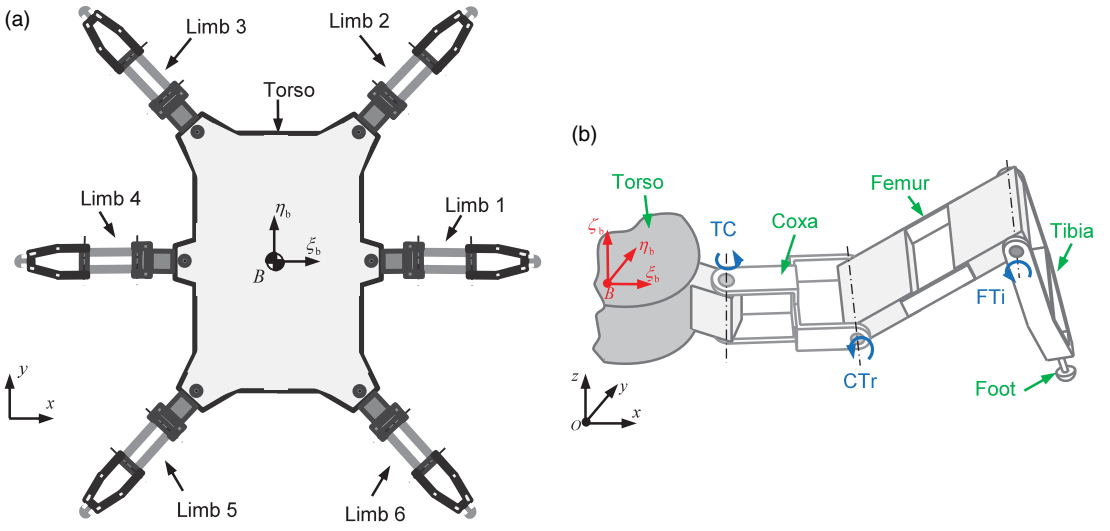

Figure 9. *Hexapod robot multibody model: (a) Multibody subsystems; (b) Representation of each limb's multibody model: green identifies the system's rigid bodies, and blue represents the active joints.*

5. Examples of application

5.1. Hexapod robotic system – ATHENA

The first example presented here is the hexapod robotic system named ATHENA, composed of six legs arranged symmetrically around the main body. A representation of the multibody system is depicted in Fig. 9a. Each limb included four bodies and has three degrees of freedom. The nomenclature for the leg's segments and joints is presented in Fig. 9b. To examine the dynamic response of the hexapod robot, it is necessary to analyze the robot as a multibody system. Thus, the multibody model of the hexapod robot is described by 25 rigid bodies and 24 joints. In terms of joints' description, 18 of them are considered active with revolute motion, while the remaining six joints fix the feet to the tibia segments [255].

For the dynamic analysis of the hexapod robotic system, specific trajectories are prescribed for all legs. For that, driving constraints are applied to each driven revolute joint. The locomotion of the hexapod robot is examined by utilizing the equation of motion derived from the multibody model. In this study, the hexapod robot adopts a tripod gait and walks across a regular surface for approximately 6 s. Each gait cycle takes 2 s to be completed. Each gait cycle takes 2 s to be completed. The limbs' trajectory is defined by a cubic spline that combines discrete points of the foot for the swing and the stance phases. The contacts between the robot's feet and the ground are modeled using the regularized approaches described in Section 4, namely those given by Eqs. (43) and (48). For the numerical resolution of the equations of motion, the Baumgarte stabilization method is utilized together with an integrator with both variable time step and order ability. The dynamic response of the hexapod system is illustrated by the diagrams showing the position and velocity of the torso, as depicted in Figs. 10a and 10b, respectively. It can be observed that the hexapod's torso moves in the longitudinal direction, and the height of the body remains stable (see Fig. 10a). In turn, the torso exhibits linear velocity, and the motion in the lateral and vertical directions is consistent throughout the computational simulations, which ultimately demonstrates the stability of the gait.

As expected, the contact forces developed between the feet and the ground influence the motion of the hexapod's limbs. Figs. 11a-f shows the plots of the normal contact forces produced during the hexapod motion. Overall, the hexapod robot produces normal contact forces of similar magnitude for all its feet. Given the model's type of gait, limbs 1, 3, and 5 must contact the ground at the same time, while the remaining limbs are in the swing phase. In the transition of the gait phases, the contact force's magnitude increases. Limb 1 supports the right-side of the hexapod robot's torso, whereas limbs 2 and

https://doi.org/10.1017/S026357472400050X Published online by Cambridge University Press

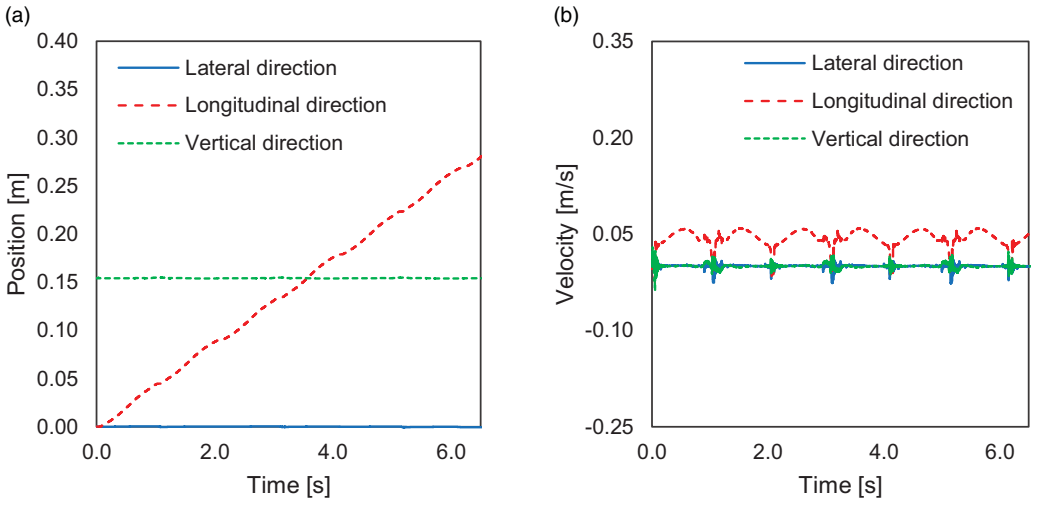

Figure 10. *Global motion of the hexapod robot: (a) Position of the torso in the lateral, longitudinal and vertical directions; (b) Velocity of the torso in the lateral, longitudinal and vertical directions.*

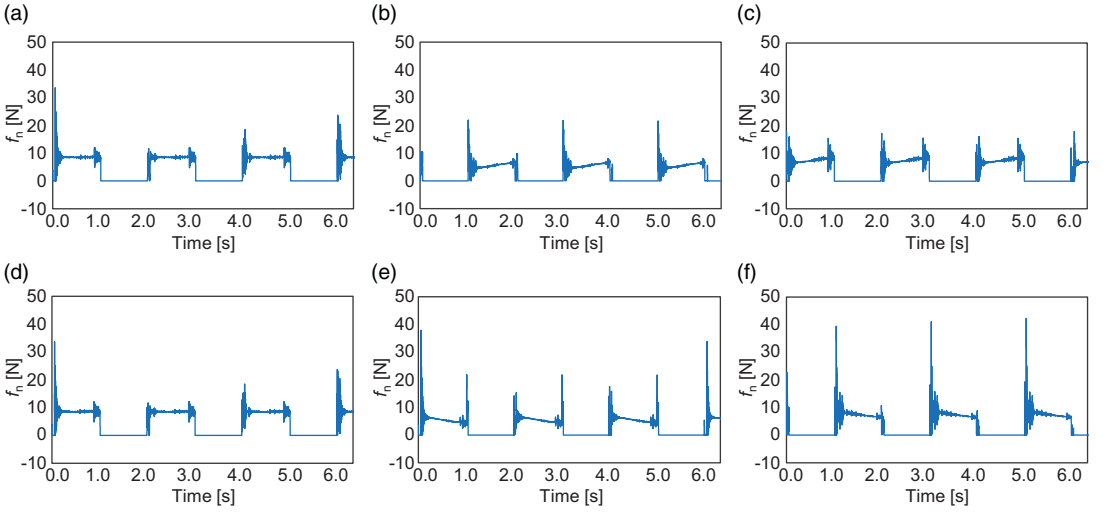

Figure 11. *Plots of the hexapod robot's normal contact forces: (a-f) Contact forces for limb 1 to 6.*

6 are in the swing phase. Thus, there is an increase of the contact force in the beginning of the stance phase, as Fig. 11a shows. The third and fifth limbs are in the model's left side. In the stance phase, the rear limb initially supports most of the weight because of the hexapod robot's motion. Furthermore, the distribution of weight gradually changes, and by the end of the stance phase, the normal contact force is higher in the third limb, as shown in the plots of Figs. 11c and e depict. This indicates that contact in the two feet occurs simultaneously. Then, the fifth limb's normal force at the contact event has a higher magnitude, which is caused by an actuation delay of the third limb. Considering that the actuation of limbs 2, 4, and 6 is identical, a similar behavior is observed (see Figs. 11b, d and f).

Considering that the same contact model is applied to all limbs, the relation between the penetration depth and the normal contact force for the second limb is presented in Fig. 12. The plot displays only the initial impacts of the second limb. It can be observed that the normal contact force's decreases during the impact events due to energy dissipation. In the stance phase, the feet are in contact with the ground.

https://doi.org/10.1017/S026357472400050X Published online by Cambridge University Press

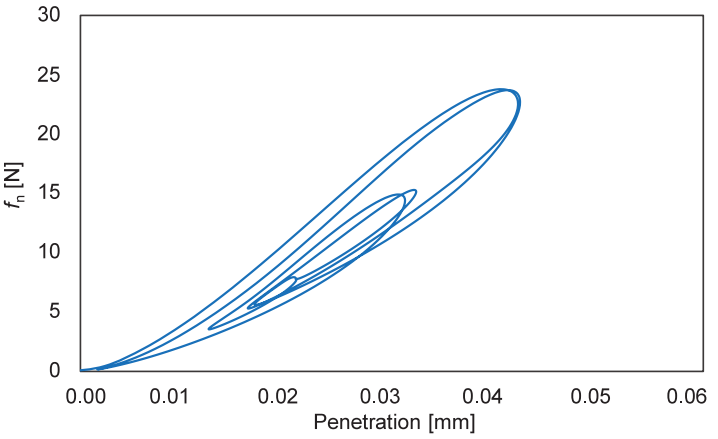

Figure 12. *Normal contact force versus penetration of the first impacts for the second limb.*

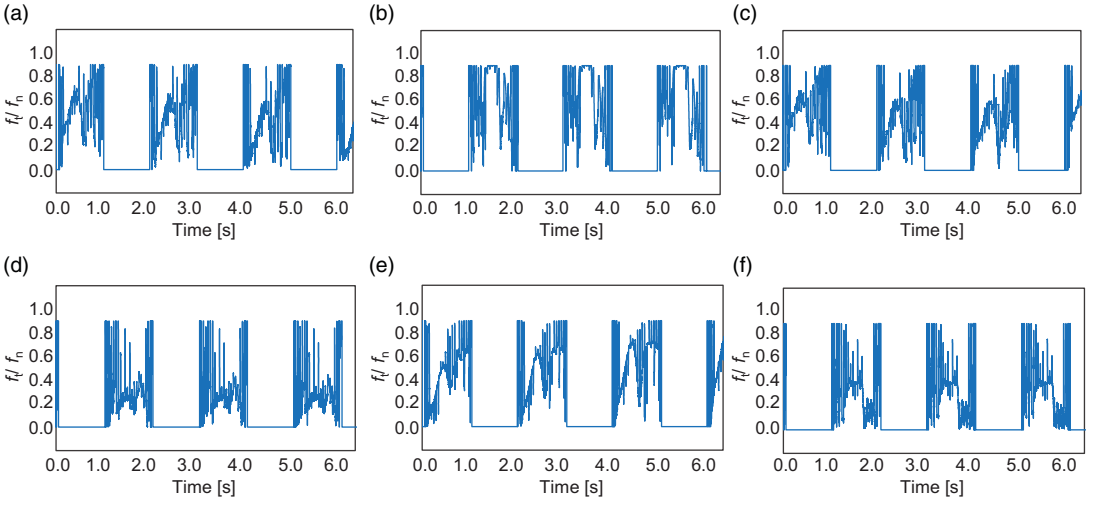

Figure 13. *Plots of the hexapod robot's tangential contact forces: (a-f) Friction forces for limb 1 to 6.*

Therefore, with the time's progression, the relation between the contact force and the relative penetration converges to a certain quantity. Due to less energy dissipation associated with the restitution phase, more energy rebounds are observed, leading to a higher variability of the normal contact force.

The motion of the hexapod robot is also influenced by the frictional forces developed between the feet and the ground. In order to better understand how friction evolves during the hexapod's motion, the ratio between the normal and friction forces of each foot is presented in Figs. 13a-f. In each gait cycle, the ratio between the friction and the normal forces does not exceed the kinetic coefficient of friction. Thus, it is considered that there is no slippage of the feet in the stance phase and the model's motion is validated. Since the friction force is directly related to the normal force, the variation of the ratio during each gait cycle is affected by the same phenomena in terms of the trajectory of the limbs.

5.2. Mobile manipulator robot – CHARMIE

The CHARMIE [256] is a human-inspired mobile manipulator robot designed to interact with humans, specifically assisting with domestic tasks. The robot is divided into five main systems: (*i*) a locomotive system using four omnidirectional wheels; (*ii*) an independent suspension system; (*iii*) an articulated

https://doi.org/10.1017/S026357472400050X Published online by Cambridge University Press

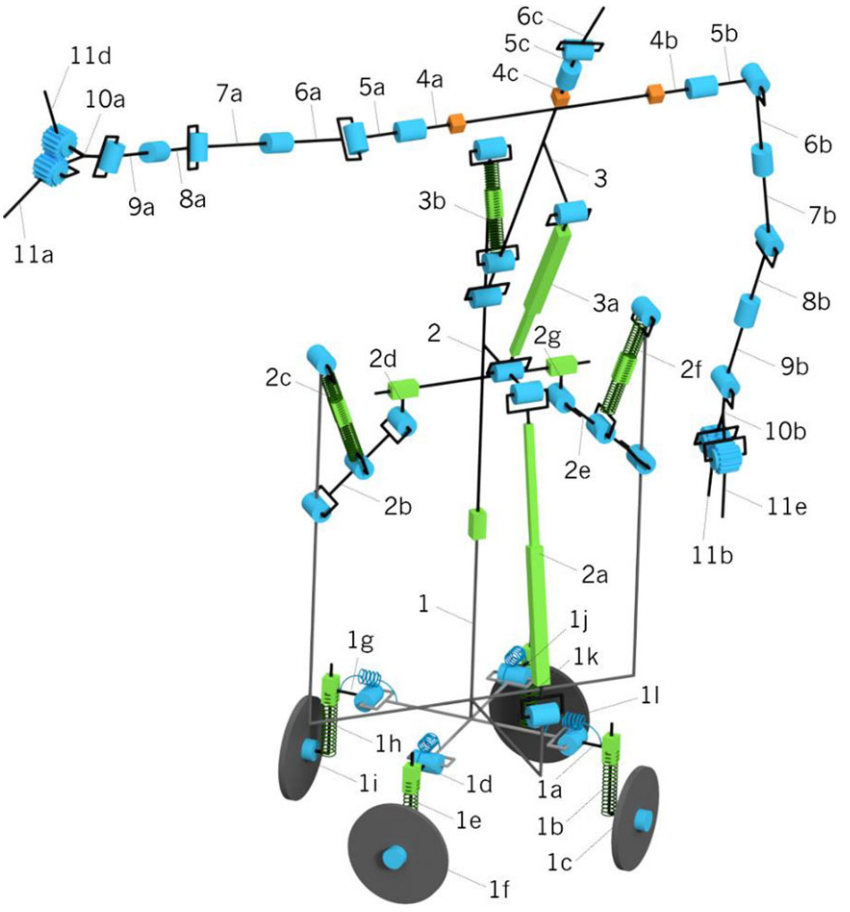

Figure 14. *Kinematic diagram showcasing the bodies and degrees of freedom of the CHARMIE robot.*

hip mechanism; (*iv*) two 7-DOF manipulator arms; and (*v*) the robot's head. This robot is modelled as a multibody system with 45 bodies and 54 joints (Fig. 14), assembled in a configuration which results in a total of 36 degrees of freedom (including the six degrees of freedom that allow the robot to navigate through space). The key bodies in CHARMIE's structure are 1 the base, 2 the hip, 3 the trunk, 4a-10a the right arm, 4b-10b the left arm, and 4c-6c the robot's head.

The CHARMIE multibody model is represented by a kinematic tree (Fig. 15), where the branches are treated as serial systems using recursive algorithms. First, the forward kinematics of each link are modeled from the base to the end-effector. Subsequently, a Newton–Euler formulation is employed to perform the dynamic analysis. The closed and overconstrained loops (connecting the link pairs 1-2 and 2-3) necessitated additional formulation to solve both the kinematics and dynamics.

The interaction of the CHARMIE system with its surroundings can be analyzed using forward dynamics. These interactions are collisions with obstacles, the wheel-floor contact dynamics, and the manipulation of intended objects. The multibody system has been implemented into Python [18]. The numpy library was used to assist in solving mathematical operations, while the matplotlib library assisted in generating the graphical outputs of the simulator (Fig. 16). The resulting code is hardware-independent and can be implemented into the robot's embedded computer.

The equations of motion describing the behavior of the robot's bodies are computed to create the simulator. These equations take as inputs the physical properties of the bodies (mass, inertia, and geometry) and joints (orientation, joint type, and joint placement). The simulation environment incorporates the multibody model of the robot, a flat floor plane, two tables with which the robot can collide, and

https://doi.org/10.1017/S026357472400050X Published online by Cambridge University Press

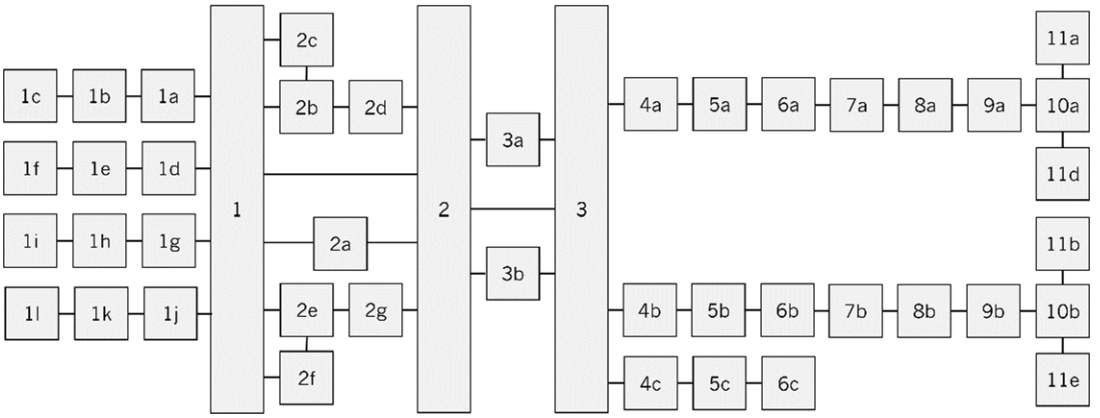

Figure 15. *Kinematic tree representing CHARMIE's multibody system.*

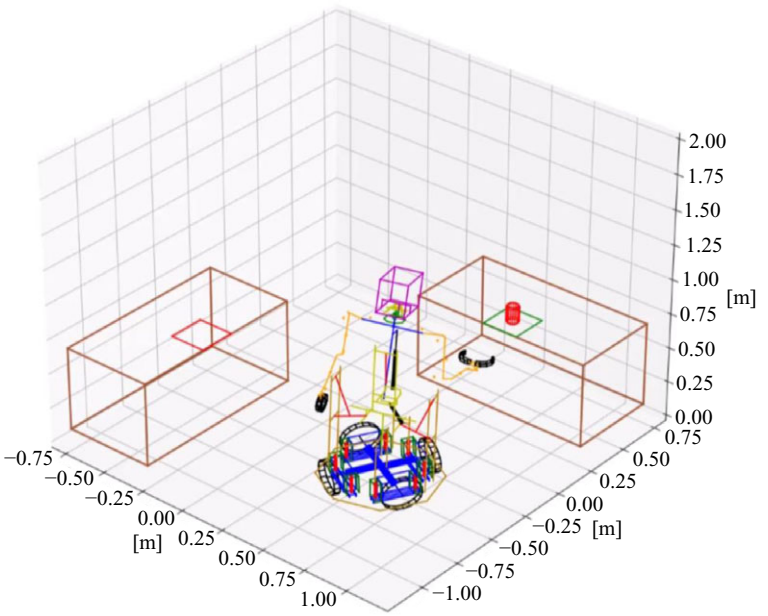

Figure 16. *Simulation environment for testing the CHARMIE robot.*

a cylindrical body representing a can which will be the target of manipulation of the robot. The position of the robot, the tables, and the cylindrical body can be randomized for the training of a neural network solution. The results derived from both the kinematic and dynamic analyses of the developed approach undergo validation through a comparison with outcomes generated by commercial software, namely the Visual Nastran 4D. The same motion was tested for both simulation environments. As it was expected, both methodologies give similar outcomes, as it is visible in the plots of Figs. 17 and 18, which show a very good agreement between the overall results obtained with present approach and commercial software. Furthermore, the simulator's computational efficiency was evaluated utilizing four different models: a 2-DOF Arm, a 4-DOF Arm, a 6-DOF Arm, and the CHARMIE Robot. These models were simulated, without a graphical interface, in PyCharm on a computer with an AMD Ryzen 5 5600X 6-Core Processor 3.70 GHz, efficiency of which is presented in Table II.

https://doi.org/10.1017/S026357472400050X Published online by Cambridge University Press

Table II. *Comparison of the computational effort for 1000 time-steps of simulation for different models.*

Model	2-DOF Arm	4-DOF Arm	6-DOF Arm	CHARMIE
Kinematic Model	0.211 s	0.269 s	0.325 s	2.409 s
Dynamic Model	0.482 s	0.715 s	0.947 s	7.856

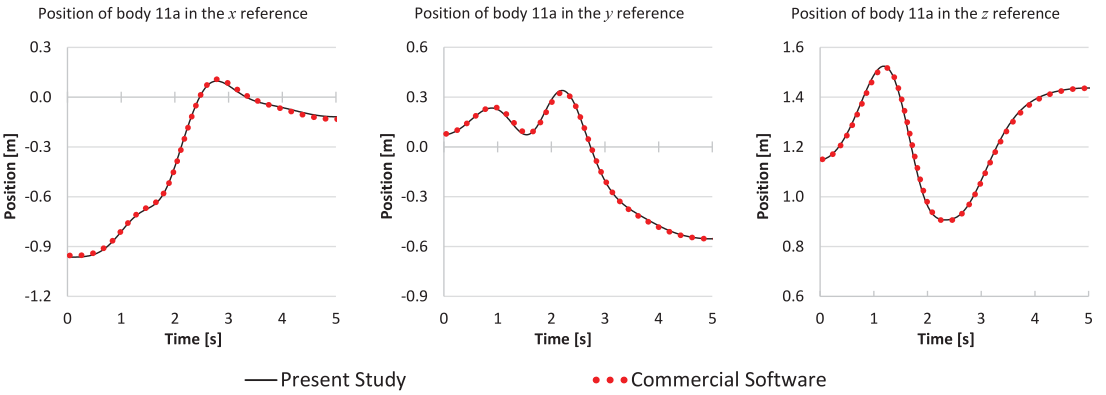

Figure 17. *Comparison between the results for the forward kinematics of the robot's end-effector for the simulator utilized in the present study and a commercial software (Visual nastran 4D).*

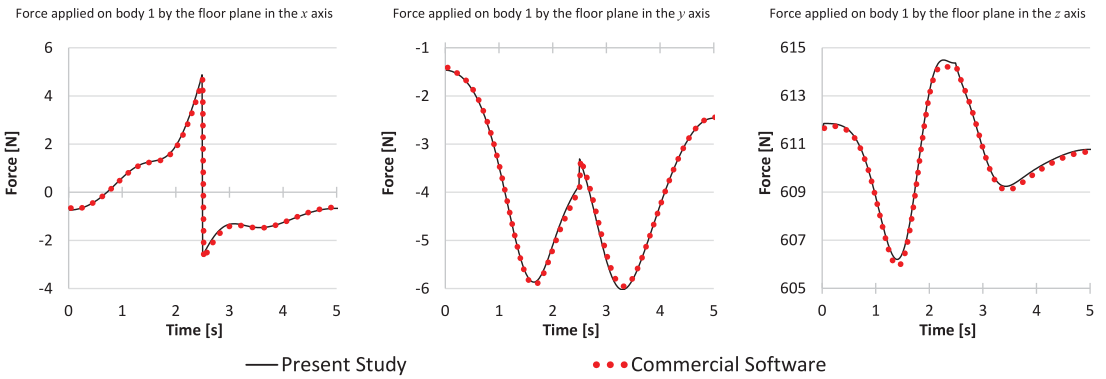

Figure 18. *Comparison between the results for the inverse dynamics of the robot's end-effector for the simulator utilized in the present study and a commercial software (Visual nastran 4D).*

6. Concluding remarks

In this paper, the important problem of modeling and simulation multibody systems in particular field of robotics is revisited. Special attention was given to the cases that involve contact-impact scenarios in their dynamic response. Multibody dynamics methodologies are quite effective tools to model and simulate robotic systems that experience contact conditions with the surrounding environment, namely those that occur between feet and ground in robots' locomotion. When dealing with these challenging problems, it is essential to properly address the large displacement of the robot bodies, as well as the demanding aspects associated with the numerical and computational implementation of the collisions in dynamical systems. Moreover, a general methodology based on the Newton–Euler method was used to represent the motion of robotic systems. The fundamental kinematic and dynamic characteristics necessary to derive the equations of motion were outlined. Additionally, a numerical procedure suitable

https://doi.org/10.1017/S026357472400050X Published online by Cambridge University Press

for solving these equations was presented. The demanding issue of modeling contact-impact events in dynamical systems encompasses two primary tasks: contact detection and contact resolution.

To accurately model collisions, the contact kinematic properties are established based on the geometry of the contacting bodies, facilitating the contact detection task. Subsequently, continuous contact force models are employed to represent contact dynamics, encompassing both normal and tangential contact directions. In the realm of normal contact forces, this discussion delves into regularized models rooted in the established Hertzian contact theory, augmented with a dissipative term. Similarly, various regularized friction force models, based on Coulomb's friction law, were scrutinized. These models prove to be highly effective, offering a balance between accuracy and stability in resolving the equations of motion. Two illustrative examples of applications within the framework of multibody systems methodologies were discussed. These examples serve to emphasize the essential aspects associated with the modeling of contact-impact events in robotics. Particular attention was given to the dynamic behavior of the systems, focusing on aspects of performance and stability.

Future developments in the realm of multibody dynamics for robotic systems with collisions may encompass: (*i*) identification and estimation of contact parameters by exploring methods to identify and estimate contact parameters in intricate scenarios, enhancing the understanding of contact interactions; (*ii*) benchmark problem development by creating benchmark problems to evaluate the effectiveness of existing techniques in handling contact-impact events; (*iii*) analysis of large contact areas by investigating contact problems with extensive contact areas, addressing challenges that arise when dealing with such complex scenarios; (*iv*) accelerating contact detection by developing techniques to accelerate the contact detection process, especially in situations involving multiple potential contacts. Absolutely, addressing these aspects can indeed contribute significantly to both the efficiency of simulations and real-time applications, as well as foster advancements in methodologies. By enhancing the ability to identify and estimate contact parameters, creating benchmark problems, tackling large contact areas, and accelerating contact detection, we can refine and optimize the modeling and simulation of robotic systems with collisions. This, in turn, will positively influence the development and performance of robotic technologies across diverse applications.

Author contributions. M.R. Silva, F. Novais, and P. Flores conceived and designed the study. J. Coelho, F. Gonçalves, and P. Flores developed methodology, J. Coelho and F. Gonçalves implemented solutions, J. Coelho, F. Gonçalves, and P. Flores analyzed results. M.R. Silva, J. Coelho, F. Gonçalves, F. Novais, and P. Flores wrote article.

Financial support. The first, second and third authors acknowledge the support from Portuguese Foundation for Science and Technology (FCT) through the PhD grants (2021.04840.BD, SFRH/BD/145818/2019, and SFRH/BD/145993/2019), with funds from the Portuguese Ministry of Science, Technology and Higher Education and the European Social Fund through the *Programa Operacional Regional Norte*. This work has been supported by the Portuguese Foundation for Science and Technology, under the national support to RD units grant, with the reference project UIDB/04436/2020 and UIDP/04436/2020.

Competing interests. The authors declare no competing interests exist.

Ethical approval. Not applicable.

References

[1] C. Antonya and R. G. Boboc, "Computational efficiency of multi-body systems dynamic models," *Robotica* **39**(12), 2333–2348 (2021).
[2] Z. Li, C. Li, S. Li, S. Zhu and H. Samani, "A sparsity-based method for fault-tolerant manipulation of a redundant robot," *Robotica* **40**(10), 3396–3414 (2022).
[3] P. Zhang, J. Zhang and A. Elsabbagh, "Fuzzy radial-based impedance controller design for lower limb exoskeleton robot," *Robotica* **41**(1), 326–345 (2023).
[4] P. You, Z. Liu and Z. Ma, "Multibody dynamic modeling and analysis of cable-driven snake robot considering clearance and friction based on ALE method," *Mech Mach Theory* **184**, 105313 (2023).
[5] A. Grazioso, A. Ugenti, R. Galati, G. Mantriota and G. Reina, "Modeling and validation of a novel tracked robot via multibody dynamics," *Robotica* **41**(10), 3211–3232 (2023).

https://doi.org/10.1017/S026357472400050X Published online by Cambridge University Press

[6] E. Mucchi, S. Fiorati, R. Di Gregorio and G. Dalpiaz, "Multibody modeling and vibration testing of 3R planar manipulators: Effects of flexible installation frames," *Robotica* **31**(8), 1209–1220 (2013).
[7] L. Bascetta, G. Ferretti and B. Scaglioni, "Closed form Newton-Euler dynamic model of flexible manipulators," *Robotica* **35**(5), 1006–1030 (2017).
[8] X. Chang, H. An and H. Ma, "Modeling and base parameters identification of legged robots," *Robotica* **40**(3), 747–761 (2022).
[9] C. Vasileiou, A. Smyrli, A. Drogosis and E. Papadopoulos, "Development of a passive biped robot digital twin using analysis, experiments, and a multibody simulation environment," *Mech Mach Theory* **163**, 104346 (2021).
[10] M. Safartoobi, M. Dardel and H. M. Daniali, "Gait cycles of passive walking biped robot model with flexible legs," *Mech Mach Theory* **159**, 10429 (2021).
[11] M. Kim, W. Moon, D. Bae and I. Park, "Dynamic simulations of electromechanical robotic systems driven by DC motors," *Robotica* **22**(5), 523–531 (2004).
[12] R. Ingrosso, D. De Palma, G. Avanzini and G. Indiveri, "Dynamic modeling of underwater multi-hull vehicles," *Robotica* **38**(9), 1682–1702 (2020).
[13] J. Coelho, F. Ribeiro, B. Dias, G. Lopes and P. Flores, "Trends in the control of hexapod robots: A survey," *Robotics* **10**(3), 100 (2021).
[14] D. Di Vito, D. De Palma, E. Simetti, G. Indiveri and G. Antonelli, "Experimental validation of the modeling and control of a multibody underwater vehicle manipulator system for sea mining exploration," *J Field Robot* **38**(2), 171–191 (2021).
[15] A. Wadi and S. Mukhopadhyay, "A novel localization-free approach to system identification for underwater vehicles using a universal adaptive stabilizer," *Ocean Eng* **274**, 114013 (2023).
[16] J. H. Kim, J. Yang and K. Abdel-Malek, "Planning load-effective dynamic motions of highly articulated human model for generic tasks," *Robotica* **27**(05), 739–747 (2009).
[17] P. Zhang and J. Zhang, "Lower limb exoskeleton robots' dynamics parameters identification based on improved beetle swarm optimization algorithm," *Robotica* **40**(8), 2716–2731 (2022).
[18] F. Gonçalves, T. Ribeiro, A. F. Ribeiro, G. Lopes and P. Flores, "Dynamic Modeling of a Human-Inspired Robot Based on a Newton-Euler Approach," **In:** *CISM International Centre for Mechanical Sciences, Courses and Lectures*, Vol. **606** (Springer, Cham, 2022) pp. 79–90.
[19] F. Gonçalves, T. Ribeiro, A. F. Ribeiro, G. Lopes and P. Flores, "A recursive algorithm for the forward kinematic analysis of robotic systems using euler angles," *Robotics* **11**(1), 15 (2022).
[20] A. A. Transeth, K. Y. Pettersen and P. Liljebäck, "A survey on snake robot modeling and locomotion," *Robotica* **27**(7), 999–1015 (2009).
[21] G. Vossoughi, H. Pendar, Z. Heidari and S. Mohammadi, "Assisted passive snake-like robots: Conception and dynamic modeling using Gibbs-Appell method," *Robotica* **26**(3), 267–276 (2008).
[22] S. M. Mirtaheri and H. Zohoor, "Efficient formulation of the Gibbs-Appell equations for constrained multibody systems," *Multibody Syst Dyn* **53**(3), 303–325 (2021).
[23] A. Talaeizadeh, M. Forootan, M. Zabihi and H. N. Pishkenari, "Comparison of kane's and Lagrange's methods in analysis of constrained dynamical systems," *Robotica* **38**(12), 2138–2150 (2020).
[24] F. Saunders, E. Golden, R. D. White and J. Rife, "Experimental verification of soft-robot gaits evolved using a lumped dynamic model," *Robotica* **29**(6), 823–830 (2011).
[25] J. Zou, Y. Lin, C. Ji and H. Yang, "A reconfigurable omnidirectional soft robot based on caterpillar locomotion," *Soft Robot* **5**(2), 164–174 (2018).
[26] J. Jia, P. Cheng, Y. Ye, Q. Xie and C. Wu, "A novel soft-rigid wheeled crawling robot with high payload and passing capability," *Robotica* **40**(11), 3930–3951 (2022).
[27] A. Banerjee, A. Chanda and R. Das, "Historical origin and recent development on normal directional impact models for rigid body contact simulation: A critical review," *Arch Comput Method Eng* **24**(2), 397–422 (2017).
[28] L. Skrinjar, J. Slavič and M. Boltežar, "A review of continuous contact-force models in multibody dynamics," *Int J Mech Sci* **145**, 171–187 (2018).
[29] M. Machado, P. Moreira, P. Flores and H. M. Lankarani, "Compliant contact force models in multibody dynamics: Evolution of the hertz contact theory," *Mech Mach Theory* **53**, 99–121 (2012).
[30] F. Marques, P. Flores, J. C. Pimenta Claro and H. M. Lankarani, "A survey and comparison of several friction force models for dynamic analysis of multibody mechanical systems," *Nonline Dynam* **86**(3), 1407–1443 (2016).
[31] F. Marques, P. Flores, J. C. P. Claro and H. M. Lankarani, "Modeling and analysis of friction including rolling effects in multibody dynamics: A review," *Multibody Syst Dyn* **45**(2), 223–244 (2019).
[32] E. Pennestrì, V. Rossi, P. Salvini and P. P. Valentini, "Review and comparison of dry friction force models," *Nonlinear Dyn* **83**(4), 1785–1801 (2016).
[33] M. K. Vukobratović and V. Potkonjak, "Dynamics of contact tasks in robotics. Part I: General model of robot interacting with environment," *Mech Mach Theory* **34**(6), 923–942 (1999).
[34] L. Saraiva, M. Rodrigues da Silva, F. Marques, M. Tavares da Silva and P. Flores, "A review on foot-ground contact modeling strategies for human motion analysis," *Mech Mach Theory* **177**, 105046 (2022).
[35] M. Vukobratovic, V. Potkonjak and V. Matijevic, "Contribution to the study of dynamics and dynamic control of robots interacting with dynamic environment," *Robotica* **19**(2), 149–161 (2001).
[36] A. Loganathan and N. S. Ahmad, "A systematic review on recent advances in autonomous mobile robot navigation," *Eng Sci Tech Int J* **40**, 101343 (2023).

https://doi.org/10.1017/S026357472400050X Published online by Cambridge University Press

[37] E. D. Dottore, A. Sadeghi, A. Mondini, V. Mattoli and B. Mazzolai, "Toward growing robots: A historical evolution from cellular to plant-inspired robotics," *Front Robot AI* **5**, 16 (2018).
[38] N. Napp and R. Nagpal, "Distributed amorphous ramp construction in unstructured environments," *Robotica* **32**(2), 279–290 (2014).
[39] M. Mehdian and H. Rahnejat, "An intelligent part sorting robot in unstructured manufacturing environments," *Robotica* **10**(2), 155–164 (1992).
[40] S. M. Varedi-Koulaei, H. M. Daniali and M. Farajtabar, "The effects of joint clearance on the dynamics of the 3RRR planar parallel manipulator," *Robotica* **35**(6), 1223–1242 (2017).
[41] F. Guo, G. Cheng, S. Wang and J. Li, "Rigid-flexible coupling dynamics analysis with joint clearance for a 5-DOF hybrid polishing robot," *Robotica* **40**(7), 2168–2188 (2022).
[42] X. Tian, M. Lv, J. Sun, H. Zhao, Z. Jiang, J. Han, W. Gu and G. Cheng, "An adaptive impedance control method for polishing system of an optical mirror processing robot," *Robotica* **42**(1), 21–39 (2024).
[43] A. Zahedi, A. M. Shafei and M. Shamsi, "Kinetics of planar constrained robotic mechanisms with multiple closed loops: An experimental study," *Mech Mach Theory* **183**, 105250 (2023).
[44] N. Farhat, V. Mata, Á. Page and M. Díaz-Rodríguez, "Dynamic simulation of a parallel robot: Coulomb friction and stick-slip in robot joints," *Robotica* **28**(1), 35–45 (2010).
[45] M. Ahmadizadeh, A. M. Shafei and M. Fooladi, "A recursive algorithm for dynamics of multiple frictionless impact-contacts in open-loop robotic mechanisms," *Mech Mach Theory* **146**, 103745 (2020).
[46] W. Schiehlen, "Energy-optimal design of walking machines," *Multibody Syst Dyn* **13**(1), 129–141 (2005).
[47] H. Taheri and N. Mozayani, "A study on quadruped mobile robots," *Mech Mach Theory* **190**, 105448 (2023).
[48] A. Mahapatra, S. S. Roy and D. K. Pratihar, "Study on feet forces' distributions, energy consumption and dynamic stability measure of hexapod robot during crab walking," *Appl Math Model* **65**, 717–744 (2019).
[49] J. He and G. Ren, "A multibody dynamics approach to limit cycle walking," *Robotica* **37**(10), 1804–1822 (2019).
[50] Z. Liu, J. Gao, X. Rao, S. Ding and D. Liu, "Complex dynamics of the passive biped robot with flat feet: Gait bifurcation, intermittency and crisis," *Mech Mach Theory* **191**, 105500 (2024).
[51] Y. Tang, J. M. Zhang and D. Zhang, "A new comprehensive performance optimization approach for Earth-contact mechanism based on terrain-adaptability task," *Robotica* **41**(1), 193–214 (2023).
[52] Y. Hu and W. Guo, "A new concept of contact joint to model the geometric foot-environment contacts for efficiently determining possible stances for legged robots," *Mech Mach Theory* **162**, 104327 (2021).
[53] H. Tang, Y. Li, J. W. Zhang, D. Zhang and H. Yu, "Design and optimization of a novel sagittal-plane knee exoskeleton with remote-center-of-motion mechanism," *Mech Mach Theory* **194**, 105570 (2024).
[54] A. David and O. Bruneau, "Bipedal walking gait generation based on the sequential method of analytical potential (SMAP)," *Multibody Syst Dyn* **26**(4), 367–395 (2011).
[55] N. Kherici and Y. Mohamed Ben Ali, "Using PSO for a walk of a biped robot," *J Comput Sci* **5**(5), 743–749 (2014).
[56] P. E. Nikravesh. *Computer-aided analysis of mechanical systems* (Prentice Hall, Englewood Cliffs, New Jersey, 1988).
[57] E. Askari, P. Flores, D. Dabirrahmani and R. Appleyard, "Dynamic modeling and analysis of wear in spatial hard-on-hard couple hip replacements using multibody systems methodologies," *Nonlinear Dynam* **82**(1-2), 1039–1058 (2015).
[58] M. Rodrigues da Silva, F. Marques, M. Tavares da Silva and P. Flores, "A comparison of spherical joint models in the dynamic analysis of rigid mechanical systems: Ideal, dry, hydrodynamic and bushing approaches," *Multibody Syst Dyn* **56**(3), 221–266 (2022).
[59] P. Flores, "A methodology for quantifying the kinematic position errors due to manufacturing and assembly tolerances," *Strojniski Vestnik/J Mech Eng* **57**(6), 457–467 (2011).
[60] F. Marques, I. Roupa, M. T. Silva, P. Flores and H. M. Lankarani, "Examination and comparison of different methods to model closed loop kinematic chains using lagrangian formulation with cut joint, clearance joint constraint and elastic joint approaches," *Mech Mach Theory* **160**, 104294 (2021).
[61] P. E. Nikravesh, "Initial condition correction in multibody dynamics," *Multibody Syst Dyn* **18**(1), 107–115 (2007).
[62] M. A. Neto and J. Ambrósio, "Stabilization methods for the integration of DAE in the presence of redundant constraints," *Multibody Syst Dyn* **10**(1), 81–105 (2003).
[63] F. Marques, A. P. Souto and P. Flores, "On the constraints violation in forward dynamics of multibody systems," *Multibody Syst Dyn* **39**(4), 385–419 (2017).
[64] P. E. Nikravesh, "Newtonian-based methodologies in multi-body dynamics," *Proceed Inst Mech Engin Part K: J Multi-body Dyna* **222**(4), 277–288 (2008).
[65] J. Baumgarte, "Stabilization of constraints and integrals of motion in dynamical systems," *Comput Method Appl M* **1**(1), 1–16 (1972).
[66] C. O. Chang and P. E. Nikravesh, "An adaptive constraint violation stabilization method for dynamic analysis of mechanical systems," *J Mech Design* **107**(4), 488–492 (1985).
[67] S.-T. Lin and J.-N. Huang, "Stabilization of baumgarte's method using the runge-kutta approach," *J Mech Design* **124**(4), 633–641 (2002).
[68] P. Flores, M. Machado, E. Seabra and M. Tavares da Silva, "A parametric study on the baumgarte stabilization method for forward dynamics of constrained multibody systems," *J Comput Nonlin Dyn* **6**(1), 011019 (2011).
[69] M. Khoshnazar, M. Dastranj, A. Azimi, M. M. Aghdam and P. Flores, "Application of the bezier integration technique with enhanced stability in forward dynamics of constrained multibody systems with baumgarte stabilization method," *Eng Comput*, (2023). doi: 10.1007/s00366-023-01884-x.

[70] P. Flores and P. E. Nikravesh, "Comparison of Different Methods to Control Constraints Violation in Forward Multibody Dynamics," **In:** *International Design Engineering Technical Conferences and Computers and Information in Engineering Conference*, American Society of Mechanical Engineers, **55966**, (2013) p. V07AT10A028.
[71] R. A. Wehage and E. J. Haug, "Generalized coordinate partitioning for dimension reduction in analysis of constrained systems," *J Mech Design* **104**(1), 247–255 (1982).
[72] J. G. de Jalón and E Bayo. *Kinematic and Dynamic Simulations of Multibody Systems: The Real-Time Challenge* (Springer, New York, 1994).
[73] E. Bayo and R. Ledesma, "Augmented Lagrangian and mass-orthogonal projection methods for constrained multibody dynamics," *Nonlinear Dynam* **9**(1-2), 113–130 (1996).
[74] C. Glocker, "On frictionless impact models in rigid-body systems," *Philo Trans Royal Society: Math, Phys Eng Sci* **359**(1789), 2385–2404 (2001).
[75] M. Machado, P. Flores, J. Ambrosio and A. Completo, "Influence of the contact model on the dynamic response of the human knee joint," *Proceed Inst Mech Eng", Part K: J Multi-body Dyna* **225**(4), 344–358 (2011).
[76] P. Flores, J. Ambrósio and H. M. Lankarani, "Contact-impact events with friction in multibody dynamics: Back to basics," *Mech Mach Theory* **184**, 105305 (2023).
[77] P. Flores and J. Ambrósio, "On the contact detection for contact-impact analysis in multibody systems," *Multibody Syst Dyn* **24**(1), 103–122 (2010).
[78] H. M. Lankarani and P. E. Nikravesh, "A contact force model with hysteresis damping for impact analysis of multibody systems," *J Mech Design* **112**(3), 369–376 (1990).
[79] E. Askari, P. Flores, D. Dabirrahmani and R. Appleyard, "A review of squeaking in ceramic total hip prostheses," *Tribol Int* **93**, 239–256 (2015).
[80] J. Costa, J. Peixoto, P. Moreira, P. Flores, A. P. Souto and H. M. Lankarani, "Influence of the hip joint modeling approaches on the kinematics of human gait," *J Tribo* **138**(3), 031201 (2016).
[81] F. Pfeiffer, "Non-smooth engineering dynamics," *Meccanica* **51**(12), 3167–3184 (2016).
[82] D. S. Lopes, M. T. Silva, J. A. Ambrósio and P. Flores, "A mathematical framework for rigid contact detection between quadric and superquadric surfaces," *Multibody Syst Dyn* **24**(3), 255–280 (2010).
[83] M. Machado, P. Flores and J. Ambrósio, "A lookup-table-based approach for spatial analysis of contact problems," *J Comput Nonlin Dyn* **9**(4), 041010 (2014).
[84] F. Marques, H. Magalhães, B. Liu, J. Pombo, P. Flores, J. Ambrósio, J. Piotrowski and S. Bruni, "On the generation of enhanced lookup tables for wheel-rail contact models," *Wear* **434-435**, 202993 (2019).
[85] R. G. Moreno, F. Marques, E. C. Abad, J. M. Alonso, P. Flores and C. Castejon, "Enhanced modelling of planar radial-loaded deep groove ball bearings with smooth-contact formulation," *Multibody Syst Dyn* **60**(1), 121–159 (2024).
[86] M. Machado, P. Flores, J. C. P. Claro, J. Ambrósio, M. Silva, A. Completo and H. M. Lankarani, "Development of a planar multi-body model of the human knee joint," *Nonlinear Dynam* **60**(3), 459–478 (2010).
[87] P. Flores and J. Ambrósio, "Revolute joints with clearance in multibody systems," *Comput Struc* **82**(17-19), 1359–1369 (2004).
[88] P. Flores, J. Ambrósio, J. C. P. Claro and H. M. Lankarani, "Influence of the contact-impact force model on the dynamic response of multi-body systems," *Proceed Inst Mech Eng, Part K: J Multi-body Dyn* **220**(1), 21–34 (2006).
[89] C. Glocker, "Concepts for modeling impacts without friction," *Acta Mech* **168**(1-2), 1–19 (2004).
[90] J. Pombo and J. Ambrósio, "Application of a wheel-rail contact model to railway dynamics in small radius curved tracks," *Multibody Syst Dyn* **19**(1-2), 91–114 (2008).
[91] W. Schiehlen and R. Seifried, "Three approaches for elastodynamic contact in multibody systems," *Multibody Syst Dyn* **12**(1), 1–16 (2004).
[92] P. Flores, M. Machado, M. T. Silva and J. M. Martins, "On the continuous contact force models for soft materials in multibody dynamics," *Multibody Syst Dyn* **25**(3), 357–375 (2011).
[93] P. Flores, "Contact mechanics for dynamical systems: A comprehensive review," *Multibody Syst Dyn* **54**(2), 127–177 (2022).
[94] P. E. Nikravesh and M. Poursina, "Determination of effective mass for continuous contact models in multibody dynamics," *Multibody Syst Dyn* **58**(3-4), 253–273 (2023).
[95] S. Ding, B. Jian, Y. Zhang, R. Xia and G. Hu, "A normal contact force model for viscoelastic bodies and its finite element modeling verification," *Mech Mach Theory* **181**, 105202 (2023).
[96] K. Wang and Q. Tian, "A nonsmooth method for spatial frictional contact dynamics of flexible multibody systems with large deformation," *Int J Numer Meth Eng* **124**(3), 752–779 (2023).
[97] G. Wang, D. Ma, C. Liu and Y. Liu, "Development of a compliant dashpot model with nonlinear and linear behaviors for the contact of multibody systems," *Mech Syst Signal Pr* **185**, 109785 (2023).
[98] J. Ma, J. Wang, Y. Han, S. Dong, L. Yin and Y. Xiao, "Towards data-driven modeling for complex contact phenomena via self-optimized artificial neural network methodology," *Mech Mach Theory* **182**, 3023 (2023).
[99] H. M. Lankarani, "A poisson-based formulation for frictional impact analysis of multibody mechanical systems with open or closed kinematic chains," *J Mech Design* **122**(4), 489–497 (2000).
[100] H. M. Lankarani and M. F. O. S. Pereira, "Treatment of impact with friction in planar multibody mechanical systems," *Multibody Syst Dyn* **6**(3), 203–227 (2001).
[101] S. J. Piazza and S. L. Delp, "Three-dimensional dynamic simulation of total knee replacement motion during a step-up task," *J Biomech Eng* **123**(6), 599–606 (2001).
[102] F. Pfeiffer and C. Glocker. *Multibody Dynamics with Unilateral Constraints* (John Wiley and Sons, New York, 1996).

https://doi.org/10.1017/S026357472400050X Published online by Cambridge University Press

[103] C. H. Glocker and F. Pfeiffer, "Dynamical systems with unilateral contacts," *Nonlinear Dynam* **3**(4), 245–259 (1992).
[104] R. I. Leine, D. H. Van Campen and C. H. Glocker, "Nonlinear dynamics and modeling of various wooden toys with impact and friction," *J Vib Control* **9**(1-2), 25–78 (2003).
[105] T. Klisch, "Contact mechanics in multibody dynamics," *Mech Mach Theory* **34**(5), 665–675 (1999).
[106] P. Ravn, "A continuous analysis method for planar multibody systems with joint clearance," *Multibody Syst Dyn* **2**(1), 1–24 (1998).
[107] P. Peng, C. Di, L. Qian and G. Chen, "Parameter identification and experimental investigation of sphere-plane contact impact dynamics"2," *Exp Techniques* **41**(5), 547–555 (2017).
[108] S. Chen and Z. Zhang, "Modification of friction for straightforward implementation of friction law," *Multibody Syst Dyn* **48**(2), 239–257 (2020).
[109] Z. Qian, D. Zhang and C. Jin, "A regularized approach for frictional impact dynamics of flexible multi-link manipulator arms considering the dynamic stiffening effect," *Multibody Syst Dyn* **43**(3), 229–255 (2018).
[110] F. Marques, Łukasz Woliński, M. Wojtyra, P. Flores and H. M. Lankarani, "An investigation of a novel LuGre-based friction force model," *Mech Mach Theory* **166**, 104493 (2021).
[111] D. Verscheure, I. Sharf, H. Bruyninckx, J. Swevers and J. De Schutter, "Identification of contact parameters from stiff multi-point contact robotic operations," *Int J Rob Res* **29**(4), 367–385 (2010).
[112] A. Roy and J. A. Carretero, "A damping term based on material properties for the volume-based contact dynamics model," *Int J Nonlin Mech* **47**(3), 103–112 (2012).
[113] F. Pfeiffer and C. Glocker, "Contacts in multibody systems," *J Appl Math Mech* **64**(5), 773–782 (2000).
[114] F. Pfeiffer, "On non-smooth multibody dynamics," *Proceed Inst Mech Eng Part K: J Multi-body Dyn* **226**(2), 147–177 (2012).
[115] B. M. Kwak, "Complementarity problem formulation of three-dimensional frictional contact," *J Appl Mech* **58**(1), 134–140 (1991).
[116] J.-S. Pang and J. C. Trinkle, "Complementarity formulations and existence of solutions of dynamic multi-rigid-body contact problems with coulomb friction," *Math Program* **73**(2), 199–226 (1996).
[117] F. Pfeiffer, "The idea of complementarity in multibody dynamics," *Arch Appl Mech* **72**(11), 807–816 (2003).
[118] A. Signorini, Sopra alcune questioni di elastostatica, (Atti della società italiana per il progresso delle scienze, (1993).
[119] J. C. Trinkle, J. A. Tzitzouris and J. S. Pang, "Dynamic multi-rigid-body systems with concurrent distributed contacts," *Philo Trans: Math, Phys Eng Sci* **359**(1789), 2575–2593 (2001).
[120] C. Studer, "Numerics of Unilateral Contacts and Friction," **In:** *Modeling and Numerical Time Integration in Non-Smooth Dynamics, (Lecture Notes in Applied and Computational Mechanics*. vol. **47** (Springer, Berlin, 2009).
[121] T. Klisch, "Contact mechanics in multibody systems," *Multibody Syst Dyn* **2**(4), 335–354 (1998).
[122] R. I. Leine, B. Brogliato and H. Nijmeijer, "Periodic motion and bifurcations induced by the painlevé paradox," *European J Mech - A/Solids* **21**(5), 869–896 (2002).
[123] F. Pfeiffer, "Impacts with friction: Structures, energy, measurements," *Arch Appl Mech* **86**(1-2), 281–301 (2016).
[124] F. Pfeiffer, "On the structure of frictional impacts," *Acta Mech* **229**(2), 629–644 (2018).
[125] P. R. Kraus and V. Kumar, "Compliant Contact Models For Rigid Body Collisions," **In:** *IEEE International Conference on Robotics and Automation*, Albuquerque, NM, USA (1997) pp. 1382–1387.
[126] E. Cataldo and R. Sampaio, "A brief review and a new treatment for rigid bodies collision models," *J Braz Soc Mech Sci* **23**(1), 63–78 (2001).
[127] J. M. Font-Llagunes, A. Barjau, R. Pàmies-Vilà and J. Kövecses, "Dynamic analysis of impact in swing-through crutch gait using impulsive and continuous contact models," *Multibody Syst Dyn* **28**(3), 257–282 (2012).
[128] A. Pazouki, M. Kwarta, K. Williams, W. Likos, R. Serban, P. Jayakumar and D. Negrut, "Compliant contact versus rigid contact: A comparison in the context of granular dynamics," *Phys Rev E* **96**(4), 042905 (2017).
[129] D. Melanz, L. Fang, P. Jayakumar and D. Negrut, "A comparison of numerical methods for solving multibody dynamics problems with frictional contact modeled via differential variational inequalities," *Comput Method Appl Mech Eng* **320**, 668–693 (2017).
[130] M. Khadiv, S. A. A. Moosavian, A. Yousefi-Koma, M. Sadedel, A. Ehsani-Seresht and S. Mansouri, "Rigid vs compliant contact: An experimental study on biped walking," *Multibody Syst Dyn* **45**(4), 379–401 (2019).
[131] K. L. Johnson. *Contact Mechanics* (Cambridge University Press, England, 1985).
[132] B. Jian, G. M. Hu, Z. Q. Fang, H. J. Zhou and R. Xia, "Comparative behavior of damping terms of viscoelastic contact force models with consideration on relaxation time," *Powder Technol* **356**, 735–749 (2019).
[133] G. Serrancolí, A. L. Kinney and B. J. Fregly, "Influence of musculoskeletal model parameter values on prediction of accurate knee contact forces during walking," *Med Eng Phys* **85**, 35–47 (2020).
[134] Q. Wan, G. Liu, C. Song, Y. Zhou, S. Ma and R. Tong, "Study on the dynamic interaction of multiple clearance joints for flap actuation system with a modified contact force model," *J Mech Sci Technol* **34**, 2701–2713 (2020).
[135] K. Kildashti, K. Dong and B. Samali, "An accurate geometric contact force model for super-quadric particles," *Comput Method Appl Mech Eng* **360**, 112774 (2020).
[136] J. Ma, G. Chen, L. Ji, L. Qian and S. Dong, "A general methodology to establish the contact force model for complex contacting surfaces," *Mech Syst Signal Process* **140**, 106678 (2020).
[137] J. Ambrósio, "A general formulation for the contact between superellipsoid surfaces and nodal points," *Multibody Syst Dyn* **50**, 415–434 (2020).

https://doi.org/10.1017/S026357472400050X Published online by Cambridge University Press

[138] B. Brogliato, J. Kovecses and V. Acary, "The contact problem in Lagrangian systems with redundant frictional bilateral and unilateral constraints and singular mass matrix. The all-sticking contacts problem," *Multibody Syst Dyn* **48**(2), 151–192 (2020).
[139] E. Paraskevopoulos, P. Passas and S. Natsiavas, "A novel return map in non-flat configuration spaces of multibody systems with impact," *Int J Solids Struct* **202**, 822–834 (2020).
[140] C. Kelly, N. Olsen and D. Negrut, "Billion degree of freedom granular dynamics simulation on commodity hardware via heterogeneous data-type representation," *Multibody Syst Dyn* **50**(4), 355–379 (2020).
[141] K. Wang, Q. Tian and H. Hu, "Nonsmooth spatial frictional contact dynamics of multibody systems," *Multibody Syst Dyn* **53**(1), 1–27 (2021).
[142] J. Wittenberg. *Dynamics of Systems of Rigid Bodies* (B. G. Teubner, Stuttgart, Germany, 1977).
[143] R. W. Wehage. *Generalized Coordinate Partitioning in Dynamic Analysis of Mechanical Systems (PhD Dissertation)* (The University of Iowa, USA, (1980).
[144] Y. A. Khulief, E. J. Haug and A. A. Shabana, Dynamic analysis of large scale mechanical systems with intermittent motion, The University of Iowa, USA, (1983). (Technical Report No. CCAD-83-10.
[145] R. A. Wehage and E. J. Haug, "Dynamic analysis of mechanical systems with intermittent motion," *J Mech Design* **104**(4), 778–784 (1982).
[146] Y. A. Khulief and A. A. Shabana, "Dynamic analysis of constrained system of rigid and flexible bodies with intermittent motion," *J Mech Trans Automat Design* **108**, 38–45 (1986).
[147] Y. A. Khulief, "Restitution and Friction in Impact Analysis of Multibody Systems Executing Plane Motion," **In:** *ASME Design Engineering Technical Conference, Paper*, Columbus, Ohio, **86-DET-50** (1986).
[148] J. A. Batlle and A. B. Condomines, "Rough collisions in multibody systems," *Mech Mach Theory* **26**(6), 565–577 (1991).
[149] H. M. Lankarani and P. E. Nikravesh, "Canonical impulse-momentum equations for impact analysis of multibody systems," *J Mech Design* **114**(1), 180–186 (1992).
[150] E. J. Haug, S. C. Wu and S. M. Yang, "Dynamics of mechanical systems with coulomb friction, stiction, impact and constraint addition-deletion – I theory," *Mech Mach Theory* **21**(5), 401–406 (1986).
[151] Y.-T. Wang and V. Kumar, "Simulation of mechanical systems with multiple frictional contacts," *J Mech Design* **116**(2), 571–580 (1994).
[152] M. Anitescu, J. F. Cremer and F. A. Potra, "Formulating three-dimensional contact dynamics problems," *Mech Struct Mach* **24**(4), 405–437 (1996).
[153] A. Ghafoor, J. S. Dai and J. Duffy, "Stiffness modelling of the soft-finger contact in robotic grasping," *J Mech Design* **126**(4), 646–656 (2004).
[154] L. Cui, J. Sun and J. S. Dai, "In-hand forward and inverse kinematics with rolling contact," *Robotica* **35**(12), 2381–2399 (2017).
[155] H. Dong, C. Qiu, D. K. Prasad, Y. Pan, J. S. Dai and I. M. Chen, "Enabling grasp action: Generalized quality evaluation of grasp stability via contact stiffness from contact mechanics insight," *Mech Mach Theory* **134**, 625–644 (2019).
[156] X.-F. Liu, G.-P. Cai, M.-M. Wang and W.-J. Chen, "Contact control for grasping a non-cooperative satellite by a space robot," *Multibody Syst Dyn* **50**(2), 119–141 (2020).
[157] K. A. Hao and J. A. Nichols, "Simulating finger-tip force using two common contact models: Hunt-crossley and elastic foundation," *J Biomech* **119**, 110334 (2021).
[158] D. W. Marhefka and D. E. Orin, "A compliant contact model with nonlinear damping for simulation of robotic systems," *IEEE Trans Syst, Man, Cyber - Part A: Syst Humans* **29**(6), 566–572 (1999).
[159] S.-S. Bi, X.-D. Zhou and D. B. Marghitu, "Impact modelling and analysis of the compliant legged robots," *Proceed Inst Mech Eng, Part K: J Multi-body Dyn* **226**(2), 85–94 (2012).
[160] Z. Chen, F. Gao, Q. Sun, Y. Tian, J. Liu and Y. Zhao, "Ball-on-plate motion planning for six-parallel-legged robots walking on irregular terrains using pure haptic information," *Mech Mach Theory* **141**, 136–150 (2019).
[161] Y. Liu and P. Ben-Tzvi, "Dynamic modeling, analysis, and comparative study of a quadruped with bio-inspired robotic tails," *Multibody Syst Dyn* **51**(2), 195–219 (2021).
[162] J. Ambrósio and P. Verissimo, "Improved bushing models for general multibody systems and vehicle dynamics," *Multibody Syst Dyn* **22**(4), 341–365 (2009).
[163] Y. Y. Tay, P. S. Bhonge and H. M. Lankarani, "Crash simulations of aircraft fuselage section in water impact and comparison with solid surface impact," *Int J Crashworthines* **20**(5), 464–482 (2015).
[164] M. Guida, A. Manzoni, A. Zuppardi, F. Caputo, F. Marulo and A. De Luca, "Development of a multibody system for crashworthiness certification of aircraft seat," *Multibody Syst Dyn* **44**(2), 191–221 (2018).
[165] Y. Y. Tay, P. Flores and H. Lankarani, "Crashworthiness analysis of an aircraft fuselage section with an auxiliary fuel tank using a hybrid multibody/plastic hinge approach," *Int J Crashworthines* **25**(1), 95–105 (2020).
[166] A. A. Shabana, K. E. Zaazaa, J. L. Escalona and J. R. Sany, "Development of elastic force model for wheel/rail contact problems," *J Sound Vib* **269**(1-2), 295–325 (2004).
[167] M. Malvezzi, E. Meli, S. Falomi and A. Rindi, "Determination of wheel-rail contact points with semianalytic methods," *Multibody Syst Dyn* **20**(4), 327–358 (2008).
[168] J. Piotrowski, B. Liu and S. Bruni, "The Kalker book of tables for non-hertzian contact of wheel and rail," *Vehicle Syst Dyn* **55**(6), 875–901 (2017).
[169] Y. Song, P. Antunes, J. Pombo and Z. Liu, "A methodology to study high-speed pantograph-catenary interaction with realistic contact wire irregularities," *Mech Mach Theory* **152**, 103940 (2020).

https://doi.org/10.1017/S026357472400050X Published online by Cambridge University Press

[170] H. Magalhães, F. Marques, B. Liu, P. Antunes, J. Pombo, P. Flores, J. Ambrósio, J. Piotrowski and S. Bruni, "Implementation of a non-hertzian contact model for railway dynamic application," *Multibody Syst Dyn* **48**(1), 41–78 (2020).
[171] E. Vollebregt, "Detailed wheel/rail geometry processing with the conformal contact approach," *Multibody Syst Dyn* **52**(2), 135–167 (2021).
[172] L. Modenese and A. T. M. Phillips, "Prediction of hip contact forces and muscle activations during walking at different speeds," *Multibody Syst Dyn* **28**(1-2), 157–168 (2012).
[173] P. Gerus, M. Sartori, T. F. Besier, B. J. Fregly, S. L. Delp, S. A. Banks, M. G. Pandy, D. D. D'Lima and D. G. Lloyd, "Subject-specific knee joint geometry improves predictions of medial tibiofemoral contact forces," *J Biomech* **46**(16), 2778–2786 (2013).
[174] E. Askari, P. Flores, D. Dabirrahmani and R. Appleyard, "Nonlinear vibration and dynamics of ceramic on ceramic artificial hip joints: A spatial multibody modelling," *Nonlinear Dynam* **76**(2), 1365–1377 (2014).
[175] E. Askari, P. Flores, D. Dabirrahmani and R. Appleyard, "A computational analysis of squeaking hip prostheses," *J Comput Nonlin Dyn* **10**(2), 024502 (2015).
[176] M. S. Shourijeh and J. McPhee, "Foot-ground contact modeling within human gait simulations: From Kelvin-Voigt to hyper-volumetric models," *Multibody Syst Dyn* **35**(4), 393–407 (2015).
[177] M. Ezati, P. Brown, B. Ghannadi and J. McPhee, "Comparison of direct collocation optimal control to trajectory optimization for parameter identification of an ellipsoidal foot-ground contact model," *Multibody Syst Dyn* **49**(1), 71–93 (2020).
[178] F. Mouzo, F. Michaud, U. Lugris and J. Cuadrado, "Leg-orthosis contact force estimation from gait analysis," *Mech Mach Theory* **148**, 103800 (2020).
[179] A. L. Schwab, J. P. Meijaard and P. Meijers, "A comparison of revolute joint clearance models in the dynamic analysis of rigid and elastic mechanical systems," *Mech Mach Theory* **37**(9), 895–913 (2002).
[180] C. Liu, K. Zhang and L. Yang, "Compliance contact model of cylindrical joints with clearances," *Act Mech Sinica/Lixue Xuebao* **21**(5), 451–458 (2005).
[181] F. Marques, F. Isaac, N. Dourado, A. P. Souto, P. Flores and H. M. Lankarani, "A study on the dynamics of spatial mechanisms with frictional spherical clearance joints," *J Comput Nonlin Dyn* **12**(5), 051013 (2017).
[182] N. Akhadkar, V. Acary and B. Brogliato, "Multibody systems with 3D revolute joints with clearances: An industrial case study with an experimental validation," *Multibody Syst Dyn* **42**(3), 249–282 (2018).
[183] J. Ambrósio and J. Pombo, "A unified formulation for mechanical joints with and without clearances/bushings and/or stops in the framework of multibody systems," *Multibody Syst Dyn* **42**(3), 317–345 (2018).
[184] F. Isaac, F. Marques, N. Dourado and P. Flores, "A finite element model of a 3D dry revolute joint incorporated in a multibody dynamic analysis," *Multibody Syst Dyn* **45**(3), 293–313 (2019).
[185] M. Cirelli, P. P. Valentini and E. Pennestrì, "A study of the non-linear dynamic response of spur gear using a multibody contact based model with flexible teeth," *J Sound Vib* **445**, 148–167 (2019).
[186] X. H. Hu, L. Cao, Y. Luo, A. Chen, E. Zhang and W. J. Zhang, "A novel methodology for comprehensive modeling of the kinetic behavior of steerable catheters," *IEEE/ASME Trans Mech* **24**(4), 1785–1797 (2019).
[187] M. Ohno and Y. Takeda, "Design of target trajectories for the detection of joint clearances in parallel robot based on the actuation torque measurement," *Mech Mach Theory* **155**, 104081 (2021).
[188] G. Kuwabara and K. Kono, "Restitution coefficient in a collision between two spheres," *Japanese J Appl Phys* **26**(8), 1230–1233 (1987).
[189] M. Renouf, F. Dubois and P. Alart, "A parallel version of the non smooth contact dynamics algorithm applied to the simulation of granular media," *J Comput Appl Math* **168**(1-2), 375–382 (2004).
[190] A. Tasora, M. Anitescu, S. Negrini and D. Negrut, "A compliant visco-plastic particle contact model based on differential variational inequalities," *Int J Nonlin Mech* **53**, 2–12 (2013).
[191] D. S. Goldobin, E. A. Susloparov, A. V. Pimenova and N. V. Brilliantov, "Collision of viscoelastic bodies: Rigorous derivation of dissipative force," *Eur Phys J E* **38**(6), 55 (2015).
[192] D. Melanz, P. Jayakumar and D. Negrut, "Experimental validation of a differential variational inequality-based approach for handling friction and contact in vehicle/granular-terrain interaction," *J Terramechanics* **65**, 1–13 (2016).
[193] J. D. Turner, "On the simulation of discontinuous functions," *J Appl Mech* **68**(5), 751–757 (2001).
[194] R. I. Leine, C. Glocker and D. H. Van Campen, "Nonlinear dynamics of the woodpecker toy," **In:** *Proceedings of the ASME Design Engineering Technical Conference*, **6C**, (2001) pp. 2629–2637.
[195] J. Slavič and M. Boltežar, "Non-linearity and non-smoothness in multi-body dynamics: Application to woodpecker toy," *Proceed Inst Mech Eng Part C: J Mech Eng Sci* **220**(3), 285–296 (2006).
[196] C. Studer, R. I. Leine and C. Glocker, "Step size adjustment and extrapolation for time-stepping schemes in non-smooth dynamics," *Int J Numer Meth Eng* **76**(11), 1747–1781 (2008).
[197] P. Flores, Contact-impact analysis in multibody systems based on the nonsmooth dynamics approach, ETH-Zurich Switzerland, (2009). (Post-Doctoral Report.
[198] K. Y. Zhang and Y. Xu, "Passive movement modeling of a woodpecker robot," *Appl Mech Mater* **415**, 23–25 (2013).
[199] P. Steinkamp, "A statically unstable passive hopper: Design evolution," *J Mech Rob* **9**(1), 011016–1 (2017).
[200] E. Corral, M. J. G. García, C. Castejon, J. Meneses and R. Gismeros, "Dynamic modeling of the dissipative contact and friction forces of a passive biped-walking robot," *Appl Sci* **10**(7), 2342 (2020).
[201] J. Galvez, A. Cosimo, F. J. Cavalieri, A. Cardona and O. Brüls, "A general purpose formulation for nonsmooth dynamics including large rotations: Application to the woodpecker toy," *J Comput Nonlin Dyn* **16**(3), 031001 (2021).

https://doi.org/10.1017/S026357472400050X Published online by Cambridge University Press

[202] R. Jankowski, "Non-linear viscoelastic modelling of earthquake-induced structural pounding," *Earthquake Eng Struc Dyn* **34**(6), 595–611 (2005).
[203] S. Muthukumar and R. DesRoches, "A hertz contact model with non-linear damping for pounding simulation," *Earthquake Eng Struc Dyn* **35**(7), 811–828 (2006).
[204] M. J. DeJong, L. De Lorenzis, S. Adams and J. A. Ochsendorf, "Rocking stability of masonry arches in seismic regions," *Earthq Spectra* **24**(4), 847–865 (2008).
[205] S. Mahmoud, X. Chen and R. Jankowski, "Structural pounding models with hertz spring and nonlinear damper," *J Appl Sci* **8**(10), 1850–1858 (2008).
[206] K. Ye, L. Li and H. Zhu, "A modified Kelvin impact model for pounding simulation of base-isolated building with adjacent structures," *Earthq Eng Eng Vib* **8**(3), 433–446 (2009).
[207] K. Ye, L. Li and H. Zhu, "A note on the hertz contact model with nonlinear damping for pounding simulation," *Earthquake Eng Struc Dyn* **38**(9), 1135–1142 (2009).
[208] O. K. Ajibose, M. Wiercigroch, E. Pavlovskaia and A. R. Akisanya, "Global and local dynamics of drifting oscillator for different contact force models," *Int J Nonlin Mech* **45**(9), 850–858 (2010).
[209] A. Banerjee, A. Chanda and R. Das, "Seismic analysis of a curved bridge considering deck-abutment pounding interaction: An analytical investigation on the post-impact response," *Earthquake Eng Struc Dyn* **46**(2), 267–290 (2017).
[210] Z. Shi and E. G. Dimitrakopoulos, "Nonsmooth dynamics prediction of measured bridge response involving deck-abutment pounding," *Earthquake Eng Struc Dyn* **46**(9), 1431–1452 (2017).
[211] V. Beatini, G. Royer-Carfagni and A. Tasora, "A non-smooth-contact-dynamics analysis of Brunelleschi's cupola: An octagonal vault or a circular dome?," *Meccanica* **54**(3), 525–547 (2019).
[212] F. Avanzini, S. Serafin and D. Rocchesso, "Interactive simulation of rigid body interaction with friction-induced sound generation," *IEEE Trans Speech Audi Pro* **13**(5), 1073–1080 (2005).
[213] S. Papetti, F. Avanzini and D. Rocchesso, "Numerical methods for a nonlinear impact model: A comparative study with closed-form corrections," *IEEE Trans Audi, Speech Lang Pro* **19**(7), 2146–2158 (2011).
[214] R. Masoudi, S. Birkett and J. McPhee, "A mechanistic multibody model for simulating the dynamics of a vertical piano action," *J Comput Nonlin Dyn* **9**(3), 061004 (2014).
[215] R. Masoudi and S. Birkett, "Experimental validation of a mechanistic multibody model of a vertical piano action," *J Comput Nonlin Dyn* **10**(6), 061004 (2015).
[216] M. Maunsbach and S. Serafin, "Non-linear contact sound synthesis for real-time audio-visual applications using modal textures"," **In:** *Proceedings of the Sound and Music Computing Conferences*, (2019) pp. 431–436.
[217] S. Timmermansa, A.-E. Ceulemans and P. Fisette, "Upright and grand piano actions dynamic performances assessments using a multibody approach," *Mech Mach Theory* **160**, 104296 (2021).
[218] E. Dintwa, M. Van Zeebroeck, E. Tijskens and H. Ramon, "Determination of parameters of a tangential contact force model for viscoelastic spheroids (fruits) using a rheometer device," *Biosyst Eng* **91**(3), 321–327 (2005).
[219] H. Kruggel-Emden, S. Wirtz and V. Scherer, "A study on tangential force laws applicable to the discrete element method (DEM) for materials with viscoelastic or plastic behavior," *Chem Eng Sci* **63**(6), 1523–1541 (2008).
[220] E. Ahmadi, H. R. Ghassemzadeh, M. Sadeghi, M. Moghaddam and S. Z. Neshat, "The effect of impact and fruit properties on the bruising of peach," *J Food Eng* **97**(1), 110–117 (2010).
[221] H. Barikloo and E. Ahmadi, "Dynamic properties of golden delicious and red delicious apple under normal contact force models," *J Texture Stud* **44**(6), 409–417 (2013).
[222] O. C. Scheffler, C. J. Coetzee and U. L. Opara, "A discrete element model (DEM) for predicting apple damage during handling," *Biosyst Eng* **172**, 29–48 (2018).
[223] S. Zhang, W. Wang, Y. Wang, H. Fu and Z. Yang, "Improved prediction of litchi impact characteristics with an energy dissipation model," *Postharvest Biol Tec* **176**, 111508 (2021).
[224] C. Glocker. *Set-Valued Force Laws: Dynamics of Non-Smooth Systems, (Lecture Notes in Applied Mechanics 1* (Springer-Verlag, Berlin, 2001).
[225] R. Leine and H. Nijmeijer, Dynamics and bifurcations of non-smooth mechanical systems (Springer, Berlin, 2004).
[226] F. Pfeiffer. *Mechanical system dynamics* (Springer, Berlin, 2008).
[227] V. Acary and B. Brogliato, "Numerical Methods for Nonsmooth Dynamical Systems, Applications in Mechanics and Electronics," **In:** *Lecture Notes in Applied and Computational Mechanics*. vol. **35** (Springer, Berlin, 2008).
[228] P. Flores and H. M. Lankarani, "*Contact Force Models for Multibody Dynamics*," In Solid Mechanics and Its Applications (Springer, Berlin, 2016).
[229] G. Gilardi and I. Sharf, "Literature survey of contact dynamics modelling," *Mech Mach Theory* **37**(10), 1213–1239 (2002).
[230] R. Seifried, W. Schiehlen and P. Eberhard, "The role of the coefficient of restitution on impact problems in multi-body dynamics," *Proceed Inst Mech Engi, Part K: J Multi-body Dyn* **224**(3), 279–306 (2010).
[231] D. E. Stewart, "Rigid-body dynamics with friction and impact," *Society Indus Appl Math* **42**(1), 3–39 (2000).
[232] J. E. Shigley and C. R. Mischke. *Mechanical engineering design* (McGraw-Hill, New York, 1989).
[233] H. Hertz, "On the contact of elastic solids," *Z Reine Angew Mathematik* **92**, 156–171 (1881).
[234] W. Goldsmith. *Impact – The Theory and Physical Behavior of Colling Solids* (Edward Around, London, England, 1960).
[235] K. H. Hunt and F. R. E. Crossley, "Coefficient of restitution interpreted as damping in vibroimpact," *J Appl Mech* **42**(2), 440–445 (1975).
[236] J. Ambrósio, "Selected challenges in realistic multibody modeling of machines and vehicles," *Iutam Bookser* **33**, 1–39 (2019).

https://doi.org/10.1017/S026357472400050X Published online by Cambridge University Press

[237] F. Marques, H. Magalhães, J. Pombo, J. Ambrósio and P. Flores, "A three-dimensional approach for contact detection between realistic wheel and rail surfaces for improved railway dynamic analysis," *Mech Mach Theory* **149**, 103825 (2020).
[238] Q. Liu, J. Cheng, D. Li and Q. Wei, "A hybrid contact model with experimental validation," *J Dyn Syst Measure Cont* **143**(9), 094501 (2021).
[239] E. Askari, "Mathematical models for characterizing non-hertzian contacts," *Appl Math Model* **90**, 432–447 (2021).
[240] E. Corral, R. G. Moreno, M. J. G. García and C. Castejón, "Nonlinear phenomena of contact in multibody systems dynamics: A review," *Nonlinear Dynam* **104**(2), 1269–1295 (2021).
[241] S. Ahmed, H. M. Lankarani and M. F. O. S. Pereira, "Frictional impact analysis in open-loop multibody mechanical systems," *J Mech Design* **121**(1), 119–127 (1999).
[242] I. M. Hutchings, "Leonardo da Vinci's studies of friction," *Wear* **360-361**, 51–66 (2016).
[243] G. Amontons, "On the resistance originating in machines"," **In:** *Proceedings of the French Royal Academy of Sciences*, (1699) pp. 206–222.
[244] C. A. Coulomb, "Théorie des machines simples, en ayant égard au frottement de leurs parties, et a la roideur dews cordages," *Memoires de Math Phys Acad Sci* **10**, 161–331 (1785).
[245] D. C. Threlfall, "The inclusion of coulomb friction in mechanisms programs with particular reference to DRAM," *Mech Mach Theory* **13**(4), 475–483 (1978).
[246] M. T. Bengisu and A. Akay, "Stability of friction-induced vibrations in multi-degree-of-freedom systems," *J Sound Vib* **171**(4), 557–570 (1994).
[247] J. A. C. Ambrósio, "Impact of rigid and flexible multibody systems: Deformation description and contact model," *Virt Nonlin Multi Syst* **103**, 57–81 (2003).
[248] P. R. Dahl, "Solid friction damping in mechanical vibrations," *AIAA J* **14**(12), 1675–1682 (1976).
[249] L. C. Bo and D. Pavelescu, "The friction-speed relation and its influence on the critical velocity of stick-slip motion," *Wear* **82**(3), 277–289 (1982).
[250] D. Karnopp, "Computer simulation of stick-slip friction in mechanical dynamic systems," *J Dyn Syst Measure Cont* **107**(1), 100–103 (1985).
[251] C. C. de Wit, H. Olsson, K. J. Åström and P. Lischinsky, "A new model for control of systems with friction," *IEEE Trans Autom Cont* **40**(3), 419–425 (1995).
[252] S. Andersson, A. Söderberg and S. Björklund, "Friction models for sliding dry, boundary and mixed lubricated contacts," *Tribol Int* **40**(4), 580–587 (2007).
[253] J. Awrejcewicz, D. Grzelczyk and Y. Pyryev, "A novel dry friction modeling and its impact on differential equations computation and Lyapunov exponents estimation," *J Vibroeng* **10**, 475–482 (2008).
[254] T. Specker, M. Buchholz and K. Dietmayer, "A new approach of dynamic friction modelling for simulation and observation," *IFAC Proceed Vol* **47**(3), 4523–4528 (2014).
[255] J. Coelho, B. Dias, G. Lopes, F. Ribeiro and P. Flores, "Development and implementation of a new approach for posture control of a hexapod robot to walk in irregular terrains," *Robotica* **42**(3), 792–816 (2024).
[256] F. Gonçalves, T. Ribeiro, A. F. Ribeiro, G. Lopes and P. Flores, "Multibody model of the human-inspired robot CHARMIE," *Multibody Syst Dyn* **60**(1), 93–120 (2024).

Cite this article: M.R. da Silva, J. Coelho, F. Gonçalves, F. Novais and P. Flores, "Multibody dynamics in robotics with focus on contact events", Robotica. https://doi.org/10.1017/S026357472400050X